Xist-dependent imprinted X inactivation and the early developmental consequences of its failure.

Maud Borensztein [1], Laurène Syx [1,2], Katia Ancelin [1], Patricia Diabangouaya [1], Christel Picard [1], Tao Liu [4], Jun-Bin Liang [4] Ivaylo Vassilev [1,2], Rafael Galupa [1], Nicolas Servant [2], Emmanuel Barillot [2], Azim Surani [3], Chong-Jian Chen [4] and Edith Heard [1].

[1] Institut Curie, PSL Research University, CNRS UMR3215, INSERM U934, 26 Rue d'Ulm, 75248 Paris Cedex 05, France

[2] Institut Curie, PSL Research University, Mines Paris Tech, Bioinformatics and Computational Systems Biology of Cancer, INSERM U900, F-75005, Paris, France

[3] Wellcome Trust Cancer Research UK Gurdon Institute, Department of Physiology, Development and Neuroscience, University of Cambridge, Tennis Court Road, Cambridge CB2 1QN, United Kingdom

[4] Annoroad Gene Technology Co., Ltd, Beijing, China

Present address

Maud Borensztein: Wellcome Trust Cancer Research UK Gurdon Institute, University of Cambridge, Tennis Court Road, Cambridge CB2 1QN, United Kingdom

Corresponding author: Edith Heard (edith.heard@curie.fr)

Abstract

The long non-coding RNA *Xist* is only expressed from the paternal X chromosome in mouse pre-implantation female embryos and leads to its transcriptional silencing. In females, absence of *Xist* leads to post-implantation lethality. Here we report that the initiation of imprinted XCI absolutely requires *Xist* using single-cell RNA-sequencing of early pre-implantation mouse embryos. Lack of paternal *Xist* leads to genome-wide transcriptional misregulation in the early blastocyst, with failure to activate the extra-embryonic pathway that is essential for post-implantation development. We also demonstrate that the expression dynamics of X-linked genes depends both on strain and parent-of-origin, as well as on location along the X chromosome, particularly at *Xist's* first "entry" sites. This study demonstrates that dosage compensation failure has an impact as early as the blastocyst stage and reveals genetic and epigenetic contributions in orchestrating the transcriptional silencing of the X chromosome during early embryogenesis.

Introduction

In mammals, differences in sex-chromosome constitution between males (XY) and females (XX) have led to the evolution of dosage compensation strategies, including transcriptional silencing of one X chromosome in females[1]. In mice, X-chromosome inactivation (XCI) first initiates in the pre-implantation embryo. The non-coding *Xist* RNA is expressed only from the paternal allele leading to paternal X (Xp) inactivation[2]. The Xp remains inactive in extra-embryonic tissues, but is reactivated in the inner cell mass followed by random XCI in the embryo proper[3,4]. In early mouse embryos, XCI has been shown to be very dynamic and its requirements, both in *cis* at the level of the X-inactivation center *(*Xic*)* and in *trans*, have been debated[5]. Imprinted XCI has been proposed to initiate *de novo*[2,9] following the onset of zygotic genome activation (ZGA) and *Xist* expression. One study proposed that Xp inactivation is initially *Xist*-independent and that *Xist* may only be required for early maintenance of silencing[6], while another reported a lack of Xp gene silencing in the absence of *Xist*[7]. These studies were all based on the analysis of just a few genes, however. Two recent single cell transcriptomic studies exploited inter-specific crosses to investigate XCI in female pre-implantation embryos[8] and differentiating ESCs[9]. These revealed that imprinted XCI indeed initiates between the 4-8-cell stage[8] and that progression of random XCI is correlated with differentiation[9]. However, the extent to which initiation of Xp-linked gene silencing is dependent on *Xist* RNA, or is influenced by strain- or parent-of-origin (*eg* imprinted X-linked genes) were not explored.

In this study, we set out to explore the precise kinetics of paternal and maternal X-linked gene expression during pre-implantation embryogenesis, using inter-specific crosses and single cell RNA sequencing (scRNAseq). This allowed us to investigate differences in the dynamics of imprinted XCI that were due to genetic background and/or to parental origin. By investigating X-linked gene expression in female embryos derived from *Xist* KO males, we

63 also demonstrate the absolute *Xist* dependence of early, imprinted XCI and report the
64 genome-wide transcriptional consequences induced by a lack of dosage compensation.
65 Overall, this study provides important insights into the transcriptional and allelic dynamics of
66 XCI, as well as the nature of the requirement for dosage compensation during the first stages
67 of mammalian development.
68

Results

Allele-specific scRNAseq during pre-implantation development

To investigate the extent and requirements of gene silencing during imprinted XCI in early embryogenesis, we profiled the expression kinetics of genes on the Xp and Xm chromosomes, using scRNAseq[10]. F1 embryos were derived from inter-specific crosses, of either wild-type (*wt*) or *Xist* paternally deleted mutant ($Xist^{pat\Delta}$) origin, between the 2-cell and blastocyst (approximately 60-64-cell) stages. Reciprocal crosses between highly polymorphic *Mus musculus castaneus* (Cast/EiJ) and *Mus musculus domesticus* (C57BL6/J) strains, herein referred to as Cast and B6 respectively, were used (Figure 1a) and a minimum of 5 embryos, and 6 single cells per stage for BC and CB *wt* embryos (Supplementary Data Set 1). Of 24,499 referenced mouse genes, 15,581 were found expressed in at least one developmental stage, including 580 X-linked genes.

We first assessed the extent to which transcriptomes of single cells were associated by stage, sex or cross, by performing principal component analyses (PCA) and hierarchical clustering (Figure 1b and Supplementary Figure 1). The primary source of variability between all cells was developmental stage, as expected based on previous studies[8], thus validating the quality of our data. Single cell transcriptomes clustered to a lesser extent by cross (BC and CB), and then by sex (XX and XY) (Supplementary Figure 1), with the differences between the sexes reaching a minimum by the 32-cell and blastocyst stages, presumably due to dosage compensation.

Timing of dosage compensation and imprinted XCI

To assess the precise timing of dosage compensation in male and female embryos, we examined autosomal and X-linked transcripts at each stage in both sexes. According to

Ohno's law[11] average X-linked gene expression should be equivalent to the expression of autosomal genes. Furthermore, equal expression of X-linked genes between females and males is expected through XCI. We compared X:Autosomes (X:A) expression ratios in single blastomeres of each sex (Figure 1c). Expected X:A ratios would be 1 in females and 0.5 in males in the absence of any dosage compensation (*ie* no X overexpression compared to autosomes, and no XCI). We found that the X:A ratios were significantly above the expected ratios as early as the 4-cell stage ($p<9*10^{-4}$ for males and females after 4-cell stage, t-test) and continued to rise until the 32-cell stage, suggesting that there is a progressive increase in expression of the X compared to autosomes at the same time as, or soon after ZGA. In females, the X:A ratio rose to 1.58, by the 32 cell stage and then significantly dropped to 1.37 by the early blastocyst stage ($p=1.96*10^{-2}$ between 32-cell and blastocyst, Kruskal-Wallis (KW) test), presumably due to XCI by this stage (see below). This suggests that X:A ratios in female blastocysts progressively reach 1, although even at the early blastocyst stage, they were still slightly higher compared to males ($p=2.03*10^{-3}$, KW), in agreement with previously published data[12;13].

We next investigated allele-specific X-linked gene expression and the timing of XCI in BC and CB female embryos. At the 2-cell stage, ZGA and massive degradation of the maternal pool of mRNAs occur. Here, transcripts are maternally biased genome-wide as expected given the residual maternal pool (Figure 1d). At subsequent stages, while autosomal transcripts reached parity for both parental genomes, with a parental ratio in blastocysts of 0.5 in both crosses, X-linked transcripts displayed maternal skewing even at the 16-cell stage. By the blastocyst stage global transcription of the Xp was significantly reduced in both crosses ($p<2.2*10^{-16}$, KW) indicating that XCI was fairly complete, as previously reported[7,8,14]. We compared the kinetics of Xp silencing for 13 X-linked genes previously analyzed by nascent RNA-FISH[14] and found that most (12/13) genes showed very similar patterns (Figure 1e and

Supplementary Figure 2), giving us confidence that our scRNAseq data, bioinformatics pipeline and expression thresholds were valid. The one gene (out of the 13) for which slightly earlier Xp silencing was found by scRNAseq compared to previous reports was *Atrx*. We confirmed that *Atrx* is inactivated on the Xp in most cells by the morula stage using RNA FISH with a gene-specific probe (Supplementary Figure 3a). We also confirmed its previously reported Xp reactivation in the blastocyst[14] (Supplementary Figure 2).

Strain-specific XCI and escape

We established an *in vivo* chromosome-wide map of X-linked gene activity between the 4-cell and blastocyst stages. Of the 580 X-linked genes expressed in our scRNAseq, we focused on the 164 (BC cross) and 134 (CB cross) most highly expressed and informative genes (RPRT>4 and expressed in at least 25% of the cells of each stage and cross with a minimum of 2 cells), for which we could establish allelic expression profiles with confidence (Supplementary Figure 3b and Figure 2 for the 125 common genes between BC and CB crosses, see Online Methods for allelic expression threshold details). A striking switch from biallelic (grey, pale pink or pale blue) expression at the 4-cell stage, to monoallelic, maternal (red) expression at the blastocyst stage can be observed for most X-linked genes. Several genes underwent only partial or no XCI (escapees) and will be discussed later. As expected, *Xist* expression was exclusively of paternal origin throughout (Figure 2 and Supplementary Figures 3b and 4). Another gene showing only paternal expression was *Fthl17f*, part of the ferritin, heavy polypeptide-like 17 family (also known as *Gm5635*), which has previously been reported to be exclusively paternally expressed and imprinted[15]. By the blastocyst stage *Fthl17f* expression was no longer detectable, presumably due to XCI (Figure 2 and Supplementary Figures 3b and 4).

We categorized genes into different groups with respect to their timing of XCI for each cross (*early ≤ 16-cell; intermediate ≤32-cell; late = blastocyst*; Figure 3a, SI Table 2 and

Online Methods). Even by the 8-cell stage, XCI is complete for a few genes (*eg Rnf12*, *Pnma5*, Figure 2 and Supplementary Figure 3b). By the blastocyst stage, Xp reached a very similar state of inactivation in both BC and CB crosses (respectively 83.5% and 84.3% of the 164 and 134 X-linked informative and expressed genes are either silenced or maternally biased at the blastocyst stage, Figures 2, 3a and 3b). However, when comparing gene expression in embryos derived from BC and CB crosses (125 common genes), marked differences were seen between crosses, with just 71.2% (89 of 125 genes) of X-linked genes falling into the same or a similar category between BC and CB crosses (*eg* early and mid or late and biased). The degree of non-consistency in silencing kinetics between crosses was evaluated if more than one developmental stage separated the same gene between BC and CB crosses (Supplementary Table 1 and Online Methods for classification details). Several genes also show strain-specific escape (Figure 3b). Some of these have previously been described[16] or reported to escape in a tissue-specific fashion at later stages of development or in somatic tissues (*eg Ddx3x, Idh3g)*[16–18]. On the other hand, several genes remain biallelically expressed even at the blastocyst stage and tend to show escape independent of strain (Figure 3b and Supplementary Table 2). Many of these also show escape in somatic tissues[19] (*eg Eif2s3x, Kdm5c*, *Utp14a*). Finally, some genes with biallelic ratios (represented as black dots in Figure 3b), correspond to genes that previously underwent Xp silencing prior to the blastocyst stage but then became re-expressed, as previously described for *Atrx*.

Xist "entry" sites and early silenced genes

We next assessed whether gene-silencing kinetics was correlated with genomic position along the X chromosome. We first focused on the 71.2% (n=89 genes) of genes with correlated kinetics between crosses and the strain-specific genes (n=48). Although early and intermediate silenced genes do tend to lie closer to the Xic compared to late silenced genes

(Figure 3c), gene silencing does not appear to occur as a simple linear gradient from the Xic according to our allele-specific expression heatmap, with the presence of some escapees close to the Xic (Figure 2). Rather, we noted that several regions across the X chromosome contain early-silenced genes (*eg Pnma5*, *Kif4, Magt1*), from which silencing appears to "spread" locally (Figure 2). A recent study in ES cells showed that *Xist* RNA initially binds to specific genomic regions (*Xist* "entry" sites) along the X chromosome, dependent on 3D proximity to the *Xist* locus[20]. This binding has been hypothesized to silence genes locally and to then spread along the rest of the X chromosome by Engreitz *et al*[20]. We found that X-linked genes lying within the predicted *Xist* entry regions (8 and 11 genes respectively in 32-cell and blastocysts), or close to (20 and 23 respectively in 32-cell and blastocysts) these regions showed the earliest silencing and strongest maternal imbalance (p=0.02 and p=0.03, KW, respectively in 32-cell and blastocysts, Figure 3d). Thus, we show that *Xist* RNA "entry" sites as defined in ESCs[20] could potentially correspond to XCI initiation sites *in vivo* during imprinted XCI.

Fully *Xist*-dependent imprinted XCI

The above findings suggested that *Xist* RNA plays an early role in triggering gene silencing during imprinted XCI. This contrasts with a previous report suggesting that initiation of imprinted XCI is *Xist*-independent[6]. Indeed, although $Xist^{pat\Delta}$ females die around E10.5, with major growth delay[21], mutant and *wt* females appear morphologically indistinguishable during pre-implantation development (data not shown). To evaluate whether XCI can be established, even in the absence of *Xist* expression as previously reported[6], we examined X-linked gene expression profiles in single cells of pre-implantation female embryos carrying a paternal *Xist* deletion ($Xist^{pat\Delta}$)[21,22]. *Xist* is normally expressed exclusively from the Xp in pre-implantation embryos[2] (Figure 2). Transcriptomes of single blastomeres

from hybrid F1 embryos (Cast females crossed with *Xist*$^{mat\Delta}$ B6 males) were compared to CB *wt* embryos from the 8-cell stage (when XCI normally initiates for some genes) to the blastocyst stage. We found similar X:A expression ratios between mutant and control female embryos up to the 32-cell stage (Figure 4a). However at the blastocyst stage, X:A ratios remained much higher in mutants compared to *wt* embryo*s* where this ratio normally decreases due to XCI ($p=1.77*10^{-4}$, KW). This indicated that Xp silencing is not initiated in *Xist*$^{pat\Delta}$ female blastocysts. Bioinformatics analysis on the *Xist*-mutant single cell transcriptomes was used to produce an allele-specific expression heatmap (see Online Methods) and, as expected given the absence of apparent dosage compensation in the mutants, we found that X-linked genes remained significantly biallelically expressed in *Xist*$^{pat\Delta}$ embryos (Figure 4b). Only 2 genes (*Rgn* and *Tktl1*) out of 122 assessed (*ie* 1.6%), showed maternal monoallelic expression in *Xist*$^{pat\Delta}$ mutant blastocysts, compared to 84.3% in CB *wt* controls. One of these, *Tktl1,* has been hypothesized to be imprinted[23]. Moreover, *Fthl17f*, a well-known imprinted gene was aberrantly expressed in *Xist*$^{pat\Delta}$ blastocysts, suggesting a lack of Xp silencing.

We thus found no evidence for *Xist*-independent XCI (Supplementary Figure 5a), even for X-linked genes previously proposed to be silenced independently of *Xist*[6] (11 out of 14 assayed by Kalantry *et al*, of which they found only *Rnf12, Abcb7* and *Atrx* to be *Xist*-dependent). Three of the genes assayed by Kalantry *et al* (*Abcb7*, *Fmr1* and *Pgk1*) showed a slight maternal bias at the 16-cell or 32-cell stages in the *Xist*$^{pat\Delta}$ cells in our study (left column, Supplementary Figure 5a). However this is probably due to variability in their parental-origin expression, also observed in CB controls (*Abcb7* and *Fmr1,* Supplementary Figures 3, 4 and 5a) rather than to Xp silencing. Instead, our data is in agreement with the Namekawa *et al* study[7] where *Xist*-dependent Xp silencing was proposed to occur based on nascent RNA-FISH on 2-cell to blastocyst stage embryos, although their study was only based

on 8 genes, 4 of which were in common with ref 5. The discrepancies between these previous studies were likely due to technical differences. The scRNAseq analysis we provide here represents chromosome-wide evidence for *Xist*-dependent gene silencing during pre-implantation embryogenesis and corroborates recent findings about *Xist*-dependent X-linked gene dosage[13].

Improper gene expression in *Xist* mutant embryos

The transcriptome of $Xist^{pat\Delta}$ embryos provided us with a unique opportunity to explore the molecular defects that occur in the absence of paternal XCI. A genome-wide differentially expressed (DE) gene analysis was performed in *wt* and $Xist^{pat\Delta}$ embryos (Supplementary Data Set 2). Expression profiles of single blastomeres of controls and mutants were still found to cluster according to developmental stage by PCA (data not shown). However, at the 8-cell and 32-cell stages, a surprisingly elevated number of DE autosomal genes (FDR<0.05) was found in $Xist^{pat\Delta}$ embryos compared to *wt* (Supplementary Figure 5b). By the blastocyst stage, when paternal XCI is normally complete in *wt* females, 30% of the total up-regulated genes in $Xist^{pat\Delta}$ embryos were found to be X-linked, corroborating an XCI defect in the absence of *Xist*. DE genes included *Tsix* (the antisense transcript to *Xist*) which is normally not expressed from the Xp at the 32-64 cell stage[24] (Figures 4b and d and Supplementary Figure 5b). The absence of *Xist* on the paternal X thus releases paternal *Tsix* repression in *cis* (without affecting the maternally imprinted *Xist/Tsix* alleles).

We explored the degree to which transcriptomes were perturbed in the *Xist* mutant embryos using Ingenuity Pathway Analysis software. We found that many aberrantly down-regulated genes in $Xist^{pat\Delta}$ female blastocysts were associated with extra-embryonic tissue pathways, embryonic growth and cell viability (Figure 4c and Supplementary Data Set 3).

Key extra-embryonic development genes that were aberrantly down-regulated included *Tead4* (trophectoderm)[25], *Sox17*[26] (primitive endoderm PrE and ExE), *Bmp4*[27] (trophectoderm TE and PrE), *Arid3a*[28] (TE specification) and *Socs3*[29] (placental development) (Figure 4d). To confirm the aberrant decrease of Sox17-positive cells in the PrE in $Xist^{pat\Delta}$ females, we performed immunofluorescence on late blastocysts (Figure 5a, c, e and g). In $Xist^{pat\Delta}$ females, fewer cells express Sox17 compared to their male littermates and the intensity of fluorescence of Sox17 is slightly decreased (Figure 5g), which corroborates the decrease in mRNA expression that we observe by scRNAseq.

Importantly, in addition to aberrant down regulation or repression of extra-embryonic genes, we also found abnormal overexpression of several pluripotency genes including *Prdm14, Esrrb* and *Tcl1* in $Xist^{pat\Delta}$ embryos. This suggested an inappropriate activation or lack of repression of such factors in the absence of XCI (Figure 4d). This is relevant to our recent findings showing that the presence of two active X chromosomes delays exit from pluripotency in ESCs, by preventing down-regulation of key genes, such as *Prdm14* or *Esrrb*[22]. Moreover, aberrant over-expression of *Prdm14, Esrrb* and *Tcl1* was observed in $Xist^{-/-}$ female ESCs induced to differentiate[22]. Intriguingly, the most significantly up-regulated gene (10 log fold change) in $Xist^{pat\Delta}$ female blastocysts was the imprinted *Rhox5* gene, also known as *Pem-1*. *Rhox5* is a member of the reproductive X-linked Hox (*Rhox*) cluster, and is expressed exclusively in the male germ line and in female (but not male) pre-implantation embryos (Xp only)[30]. Following implantation, its expression switches to the maternal allele and becomes restricted to extra-embryonic tissues[30]. The human *RHOXF1* gene that is hypothesized to be related to the murine *Rhox5*[31] shows similar sex-specific and lineage-specific expression in human pre-implantation embryos[32]. Importantly, previous *in vitro* studies demonstrated that over-expression of *Rhox5* can block differentiation of ESCs by preventing exit from pluripotency[33,34]. We validated *Rhox5* up-regulation at the protein level

using immunofluorescence and found that *Xist*^{patΔ} female blastocysts show significantly higher Rhox5 staining, particularly in the polar trophectoderm and inner cell mass region of the embryo, compared to *wt* blastocysts (Figure 5b, d, f and g). Quantification of Rhox5 immunofluorescence showed a significant increase in Rhox5 protein levels (p=0.0171, Kolmogorov-Smirnov KS test, Figure 5h) and in the number of cells stained by Rhox5 antibody (Figure 5f). This correlates well with our scRNAseq data.

We conclude that even by the early blastocyst stage, the lack of initiation of Xp inactivation in Xist^{patΔ} embryos leads to inappropriate down-regulation of several key genes involved in extra-embryonic development, overexpression of several pluripotency genes and massive overexpression of Rhox5, all of which may interfere appropriate subsequent differentiation.

Discussion

In conclusion, we have demonstrated the key role that *Xist* RNA plays in initiating imprinted XCI. Although its role in triggering random XCI had previously been established, our study provides evidence that *Xist* is clearly also essential for initiating early paternal XCI. Furthermore, our scRNAseq enabled us to identify the molecular defects in developmental pathways that emerge from this absence of dosage compensation and result in lethality a few days later. Absence of *Xist* leads to inappropriate down-regulation of extra-embryonic development, genes, lack of down-regulation of some pluripotency genes and massive overexpression of Rhox5. Together some or all of these defects must ultimately result in compromised extra-embryonic development and redirection towards what appears to be a more pluripotent state, or at least a state from which further differentiation is perturbed. Previous studies[22] and a recent scRNA analysis of differentiating ESC[9] found that XCI progression is negatively correlated with pluripotency and positively correlated with differentiation. The gene expression perturbations we observe in *Xist* mutant embryos and their subsequent lethality are consistent with this and point to some of the factors that are potentially implicated.

It is also noteworthy that the previously reported[33] aberrant induction of maternal *Xist* and Xm inactivation in extra-embryonic tissues of blastocysts carrying a maternal *Tsix* deletion demonstrates that the presence of two active X chromosomes at the blastocyst stage can still be rescued in some females, and suggests that the major defect associated with a lack of paternal XCI is initially in the extra-embryonic lineage.

In this study we also define the influence of chromosomal location, as well as genetic background and parent-of-origin, on XCI kinetics. Our finding that *Xist's* predicted initial binding sites on the X chromosome correspond to the earliest regions silenced, between the 8-16 cell stage, with evidence for local spreading in *cis* at the 32-blastocyst stage should enable

exploration of the local features that underlie the spread of silencing along the X chromosome in an *in vivo* context. Finally, our study demonstrates the critical requirement for accurate X-chromosome gene dosage during early embryo development and uncovers some of the key pathways and factors that are affected in the absence of XCI. Future dissection of these pathways and their relationship to X-linked gene dosage should provide a better understanding of the important role that even small changes in RNA and protein levels can play, not only in development but also in disease.

Acknowledgements

We thank S. Bao and N. Grabole for experimental help in single blastomere RNA sequencing and M. Guttman for sharing the *Xist* "entry" site coordinates. We are grateful to P. Gestraud and V. Sibut respectively for the help in statistical and IPA pathway analysis. We thank the pathogen-free barrier animal facility of the Institut Curie and J. Iranzo for help with the animals and the Cell and Tissue Imaging Platform - PICT-IBiSA (member of France–Bioimaging) of the Genetics and Developmental Biology Department (UMR3215/U934) of Institut Curie for help with light microscopy. We acknowledge E. Schulz, E. Nora, I. Okamoto and the members of E.H. laboratory for help, feedback and critical input. This work was funded by a fellowship of Région Ile-de-France (DIM STEMPOLE) to M.B., the Paris Alliance of Cancer Research Institutes (PACRI-ANR) to LS and ERC Advanced Investigator award (ERC-2010-AdG – No. 250367), EU FP7 grants SYBOSS (EU 7th Framework G.A. no. 242129) and MODHEP (EU 7th Framework G.A. no. 259743), La Ligue, Fondation de France, Labex DEEP (ANR-11-LBX-0044) part of the IDEX Idex PSL (ANR-10-IDEX-0001-02 PSL) and ABS4NGS (ANR-11-BINF-0001) to E.H and France Genomique National infrastructure (ANR-10-INBS-09) to EH, NS, EB.

Author Contributions

M.B., A.S. and E.H. conceived the study. M.B. performed most of the experiments. K.A. and P.D., C.P., M.B. and R.G. performed respectively the IF and the RNA-FISH experiments. T.L., J.B.L. and C.C.C. performed the single cell transcriptome library preparation and sequencing. L.S., M.B., C.C.C., I.V. N.S. and E.B. defined the data processing and bioinformatics analysis. L.S. built the computational pipeline for scRNAseq and analyzed the data with M.B. M.B. and E.H. wrote the paper.

Competing Financial Interests Statement

The authors declare no competing financial interests.

345 **References**

346 1. Lyon, M. F. Gene action in the X-chromosome of the mouse (Mus musculus L.).
347 *Nature* **190,** 372–3 (1961).
348 2. Okamoto, I. *et al.* Evidence for de novo imprinted X-chromosome inactivation
349 independent of meiotic inactivation in mice. *Nature* **438,** 369–373 (2005).
350 3. Okamoto, I., Otte, A. P., Allis, C. D., Reinberg, D. & Heard, E. Epigenetic dynamics of
351 imprinted X inactivation during early mouse development. *Science* **303,** 644–9 (2004).
352 4. Mak, W. *et al.* Reactivation of the paternal X chromosome in early mouse embryos.
353 *Science* **303,** 666–9 (2004).
354 5. Galupa, R. & Heard, E. X-chromosome inactivation: New insights into cis and trans
355 regulation. *Curr. Opin. Genet. Dev.* **31,** 57–66 (2015).
356 6. Kalantry, S., Purushothaman, S., Bowen, R. B., Starmer, J. & Magnuson, T. Evidence
357 of Xist RNA-independent initiation of mouse imprinted X-chromosome inactivation.
358 *Nature* **460,** 647–651 (2009).
359 7. Namekawa, S. H., Payer, B., Huynh, K. D., Jaenisch, R. & Lee, J. T. Two-step
360 imprinted X inactivation: repeat versus genic silencing in the mouse. *Mol. Cell. Biol.*
361 **30,** 3187–205 (2010).
362 8. Deng, Q., Ramskold, D., Reinius, B. & Sandberg, R. Single-Cell RNA-Seq Reveals
363 Dynamic, Random Monoallelic Gene Expression in Mammalian Cells. *Science (80-.).*
364 **343,** 193–196 (2014).
365 9. Chen, G. *et al.* Single-cell analyses of X Chromosome inactivation dynamics and
366 pluripotency during differentiation. *Genome Res.* **26,** 1342–1354 (2016).
367 10. Tang, F. *et al.* RNA-Seq analysis to capture the transcriptome landscape of a single
368 cell. *Nat. Protoc.* **5,** 516–35 (2010).
369 11. Brockdorff, N. & Turner, B. M. Dosage compensation in Mammals. *Cold Spring Harb*

Perspect Biol **7:a019406,** (2015).

12. Nguyen, D. K. & Disteche, C. M. Dosage compensation of the active X chromosome in mammals. *Nat. Genet.* **38,** 47–53 (2006).

13. Wang, F. *et al.* Regulation of X-linked gene expression during early mouse development by *Rlim*. *Elife* **5,** e19127 (2016).

14. Patrat, C. *et al.* Dynamic changes in paternal X-chromosome activity during imprinted X-chromosome inactivation in mice. *Proc. Natl. Acad. Sci. U. S. A.* **106,** 5198–203 (2009).

15. Kobayashi, S. *et al.* The X-linked imprinted gene family Fthl17 shows predominantly female expression following the two-cell stage in mouse embryos. *Nucleic Acids Res.* **38,** 3672–3681 (2010).

16. Calabrese, J. M. *et al.* Site-Specific Silencing of Regulatory Elements as a Mechanism of X Inactivation. *Cell* **151,** 951–963 (2012).

17. Berletch, J. B. *et al.* Escape from X Inactivation Varies in Mouse Tissues. *PLOS Genet.* **11,** e1005079 (2015).

18. Marks, H. *et al.* Dynamics of gene silencing during X inactivation using allele-specific RNA-seq. *Genome Biol.* **16,** 149 (2015).

19. Balaton, B. P. & Brown, C. J. Escape Artists of the X Chromosome. *Trends Genet.* **32,** 348–359 (2016).

20. Engreitz, J. M. *et al.* The Xist lncRNA exploits three-dimensional genome architecture to spread across the X chromosome. *Science* **341,** 1237973 (2013).

21. Marahrens, Y., Panning, B., Dausman, J., Strauss, W. & Jaenisch, R. Xist-deficient mice are defective in dosage compensation but not spermatogenesis. *Genes Dev.* **11,** 156–166 (1997).

22. Schulz, E. G. *et al.* The two active X chromosomes in female ESCs block exit from the

pluripotent state by modulating the ESC signaling network. *Cell Stem Cell* **14,** 203–216 (2014).

23. Nesbitt, A. M. Genomic imprinting of the X-linked gene transketolase-like 1 in mouse and human. *ProQuest Diss. Theses A&I.* **884624661,** (2010).

24. Lee, J. T., Davidow, L. S. & Warshawsky, D. Tsix, a gene antisense to Xist at the X-inactivation centre. *Nat. Genet.* **21,** 400–4 (1999).

25. Nishioka, N. *et al.* Tead4 is required for specification of trophectoderm in pre-implantation mouse embryos. *Mech. Dev.* **125,** 270–283 (2008).

26. Niakan, K. K. *et al.* Sox17 promotes differentiation in mouse embryonic stem cells by directly regulating extraembryonic gene expression and indirectly antagonizing self-renewal. *Genes Dev.* **24,** 312–326 (2010).

27. Graham, S. J. L. *et al.* BMP signalling regulates the pre-implantation development of extra-embryonic cell lineages in the mouse embryo. *Nat. Commun.* **5,** 5667 (2014).

28. Rhee, C. *et al.* Arid3a is essential to execution of the first cell fate decision via direct embryonic and extraembryonic transcriptional regulation. *Genes Dev.* **28,** 2219–2232 (2014).

29. Takahashi, Y. *et al.* SOCS3: An essential regulator of LIF receptor signaling in trophoblast giant cell differentiation. *EMBO J.* **22,** 372–384 (2003).

30. Kobayashi, S. *et al.* Comparison of gene expression in male and female mouse blastocysts revealed imprinting of the X-linked gene, Rhox5/Pem, at preimplantation stages. *Curr. Biol.* **16,** 166–172 (2006).

31. Li, Q., O'Malley, M. E., Bartlett, D. L. & Guo, Z. S. Homeobox gene Rhox5 is regulated by epigenetic mechanisms in cancer and stem cells and promotes cancer growth. *Mol Cancer* **10,** 63 (2011).

32. Petropoulos, S. *et al.* Single-Cell RNA-Seq Reveals Lineage and X Chromosome

Dynamics in Human Preimplantation Embryos. *Cell* **165,** 1012–1026 (2016).

33. Fan, Y., Melhem, M. F. & Chaillet, J. R. Forced expression of the homeobox-containing gene Pem blocks differentiation of embryonic stem cells. *Dev Biol* **210,** 481–96. (1999).

34. Cinelli, P. *et al.* Expression profiling in transgenic FVB/N embryonic stem cells overexpressing STAT3. *BMC Dev. Biol.* **8,** 57 (2008).

Figure Legends

Figure 1: Single cell RNA sequencing of early hybrid embryos and dosage compensation mechanisms.

(a) Schematic illustration of the single cell experiment and the harvested stages during pre-implantation mouse development. Time windows showing the persistence of maternal mRNA pool, activation of zygotic gene expression and Xp inactivation are indicated.

(b) Principal component analysis (PCA) of single oocytes and pre-implantation blastomeres (2C to blastocysts) based on scRNA data. Different stages are designed by different colors. n= 6 to 30 cells per stage (details of each single cell are in Supplementary Data Set 1).

(c) Differences in ratio of X-chromosome expression levels by autosomal expression levels, between 2-cell stage to blastocyst, using Dunn's test (Kruskal-Wallis), $p<0.001$ to **. Boxplots represent median with lower and upper quartiles.

(d) Allele-specific expression ratios for genes on autosomes (plain red, BC or yellow CB) and on X chromosomes (dashed red, BC or yellow, CB) in female single blastomeres (2-cell to blastocyst) from BC and CB crosses. Allele-specific proportion represents the number of reads mapped to the paternal genome divided by the total number of paternal and maternal reads mapped for each gene. Boxplots represent medians with lower and upper quartiles.

e) Examples of scRNA expression dynamics of three X-linked genes with their classification as "early inactivated", "intermediate inactivated" or "escapee" (as used in Patrat *et al*, 2009[14]) (see also Supplementary Figure 2). Mean percentage of parental origin transcripts is represented between oocytes and blastocyst.

Figure 2: Kinetics of silencing of X-linked genes over the entire X chromosome during imprinted XCI in different strains.

The mean allele-specific expression ratios per embryonic stage for each informative and expressed X-linked gene in 4-cell to blastocyst stage female embryos are represented as heatmaps, with strictly maternal expression (ratio ≤0.15) in red and strictly paternal expression (ratio ≥0.85) in blue. Color gradients are used in between these two values as shown in the key. Genes are ordered by genomic position (centromere top, telomere bottom). Data from CB (left) and BC (right) female embryos are shown (for thresholds see Online Method) and arrows highlight examples of early silenced or escapee genes. n= 125 informative X-linked genes in common for CB and BC crosses.

Figure 3: Different genes show different kinetics of silencing associated with their chromosomal position and *Xist* "entry" site localization.

(a) X-linked genes are clustered based on their silencing kinetics as "early" (silenced at 16-cell or earlier), "intermediate" (silenced at 32-cell), "late" (silenced at blastocyst), "biased" (maternally biased) and "escapee" (Esc, not silenced). The allelic ratio of each gene represents the number of reads mapped on the paternal genome divided by the total number of reads mapped and is represented at 4-cell, 16-cell, 32-cell and blastocyst stages from single female blastomeres. Further information is provided in Supplementary Table 1 and Online Methods. n= 137 X-linked genes (89 with consistent silencing kinetics between BC and CB crosses and 48 BC or CB-specific).

(b) Parental expression ratios of X-linked genes in female blastocysts in BC and CB strains. Each dot represents a single gene. The upper and lower sections represent data respectively from BC and CB embryos. *Xist* is represented by a red dot. Green and orange dots represent genes that escape from early XCI respectively in both strains or in strain-specific manner. Further information on escapees is found in Supplementary Table 2. n= 125 common X-linked genes.

(c) Box plot representing the distribution of the genomic distances to *Xist* locus (in Mb) for the different clusters of genes. "Transcription Start Site (TSS) of each gene has been used to measure the distance to *Xist*. $p<0.05$ corresponds to * by Dunn's test."

(d) Allelic expression of X-linked genes classified by their relative position to *Xist* "entry" sites (as identified during XCI induction in ESCs[20]): "inside" (TSS located in a *Xist* "entry" site), "next to" (TSS located less than 100 kb to an "entry" site) and "outside" (over 100 kb from an "entry" site). By Dunn's test; $p<0.05$ corresponds to *. Consistent or strain-specific genes have been used.

Boxplot represent median with lower and upper quartiles.

Figure 4: Paternal knockout of *Xist* impaired XCI, dosage compensation and differentiation pathways.

(a) Differences in ratio of X-chromosome expression levels by autosomal expression levels, between 8-cell stage to blastocyst in CB females (left panel) and $Xist^{pat\Delta}$ CB females (with a paternally inherited knock-out allele) (right panel). Boxplots represent median with lower and upper quartiles.

(b) Heatmap representing allele-specific mean expression from 8-cell to blastocyst stage of X-linked genes (as in Figure 2) in $Xist^{pat\Delta}$ mutant single cells. Strictly maternally expressed genes (allelic ratio ≤0.15) are represented in red and strictly paternally expressed genes (allelic ratio ≥0.85) in blue. Color gradients are used in between and genes have been ordered by genomic position. *Tsix* was included in the heatmap if it was expressed in at least 2 single cells per stage, even though it did not reach the expression threshold used (RPRT>4 and expressed in at least 25% of the cells of each stage and cross with a minimum of 2 cells). n = 122 genes.

(c) Major down-regulated genes and pathways detected between CB *wt* and CB $Xist^{pat\Delta}$ females extracted from Supplementary Data Set 2, using QIAGEN's Ingenuity Pathway Analysis (IPA) software (Supplementary Data Set 3). Color code for arrows, red: leads to inhibition; blue: leads to activation; orange: findings consistent with state of downstream molecule; grey: effect not predicted.

(d) Expression data of candidate genes from *wt* CB (black) and $Xist^{pat\Delta}$ CB (red) females, extracted from scRNAseq. Mean of expression is represented in Reads Per Retro-Transcribed length per million mapped reads (RPRT) during early development (8-cell to blastocyst stages). *Gapdh* gene is a control housekeeping gene. n= 4 to 30 cells per stage and genotype. By Kruskal-Wallis test; $p<0.05$ corresponds to *.

Figure 5: Abnormal Sox17 and Rhox5 patterns in *Xist*$^{pat\Delta}$ female blastocysts.

Maximum intensity projection of *wt* and *Xist*$^{pat\Delta}$ E4.25 blastocysts analyzed by immunofluorescence against Sox17 **(a, c**) or Rhox 5 **(b, d)**. Staining for Sox17 or Rhox5 is in red, DAPI is in grey. Scale bar represents 20µm. Percentage of positive cells have been assessed and summarized as the median + s.e.m. for Sox17 **(e)** and Rhox5 **(f)**. Numbers of embryos are indicated under each genotype. By Kruskal-Wallis test; $p<0.05$ and $p<0.001$ correspond respectively to * and **. Average distribution of positive single cell fluorescence was represented by measuring the corrected total cell fluorescence using ImageJ software (Fiji, NIH) for Sox17 **(g)** and Rhox5 **(h)** and tested by Kolmogorov-Smirnov test. All cells under 10,000 and 5,000 for total cell fluorescence, respectively for Sox17 and Rhox5, have been considered as negative.

Online Methods

Mouse crosses and collection of embryos

All experimental designs and procedures were in agreement with the guidelines from French legislation and institutional policies.

All BC and CB embryos were respectively derived from natural meetings between *C57BL/6J* (B6) females crossed with *CAST/EiJ* (Cast) males or by the reciprocal cross. The $Xist^{pat\Delta}$ mutant embryos ($Xist^{+/-}$) were obtained by mating between Cast females and $Xist^{-/Y}$ males (mixed background: B6D2F1: *C57BL/6J* and DBA/2J, 129S1/SvlmJ and BALB/cJ). Embryos were harvested at 2-cell, 4-cell, 8-cell, 16-cell, 32-cell and blastocyst (approximately 60 to 64-cell) stages, respectively at E1.5, E2.0, E2.25, E2.75, E3.25 and E3.5. B6 and Cast pure oocytes were collected at E0.5 after matings of females with vasectomized males (Figure 1a). The collected embryos were only included in the analysis if they showed a normal morphology and the right number of blastomeres in relation with their developmental stage.

RNA Fluorescent In Situ Hybridization

RNA FISH on preimplantation embryos was performed as previously described[3] using the intron-spanning Fosmid probe WI1-2039P10 (BacPac Consortium at Children's Hospital Oakland Research Institute) for *Atrx* and the intron-spanning plasmid probe p510 for *Xist*. Images were acquired using a wide-field Deltavision core microscope (Applied Precision – GE Healthcase) with a 60× objective (1,42 oil PL APO N) and 0.2 µm Z-sections. Images were analyzed using ImageJ software (Fiji, NIH).

Immunofluorescence staining

Immunofluorescence was carried out essentially as described previously[35] with an additional step of blocking in 3% FCS before the primary antibody incubation. Immunofluoroscence of embryos either from mutant or control male progeny were always performed in parallel and in suspension. The following antibodies were used: goat anti-mouse Pem-1 (Rhox5)/Santacruz sc-21650/1:50 and goat anti-human Sox17/R&D Systems AF1924/1:100. Images were acquired using an Inverted laser scanning confocal microscope with spectral detection (LSM700 - Zeiss) equipped with a 260nm laser (RappOpto), with a 60X objective and 2 μm Z-sections. Maximum projections and total corrected fluorescence measurements (=integrated density – (area of selected cell x mean fluorescence of background readings) were performed in Figure 5g and 5h with Image J software (Fiji, NIH) using previously described methodology[36]. The total corrected cellular fluorescence (TCCF) = integrated density – (area of selected cell × mean fluorescence of background readings), was calculated.

Single cell dissociation from pre-implantation mouse embryos

Oocytes and embryos were collected by flushing oviducts (E0.5 to E2.75) or uterus (E3.25 and E3.5) with M2 medium (Sigma). The zona pellucida was removed using acid Tyrode's solution (Sigma), and embryos were washed twice with M2 medium (Sigma). To isolate individual cells, we then incubated embryos in Ca^{2+}, Mg^{2+} free M2 medium for 5 to 20 minutes, depending on the embryonic stage. For the blastocyst stage, Ca^{2+}, Mg^{2+} free M2 free medium was replaced by a 5-minute incubation in TrypLE (Invitrogen). After incubation, each blastomere was mechanically dissociated by mouth pipetting with a thin glass capillary. Single cells were then washed 3 times in PBS/acetylated BSA (Sigma) before being manually picked into PCR tubes with a minimum amount of liquid. We either directly prepared the cDNA amplification or kept the single cells at -80°C for future preparation.

Single cell RNA amplification

PolyA$^+$ mRNA extracted from each single cell was reverse transcribed from the 3'UTR and amplified following the *Tang et al* protocol[10]. Care was taken only to process embryos and single blastomeres of the highest quality based on morphology, number of cells and on amplification yield. A total of 72 BC and 110 CB (including 113 *wt* and 69 *Xist*$^{pat\Delta}$ mutant blastomeres) have been processed and passed quality controls.

Quality and sex determination

After cDNA amplification and before size selection and library preparation, the quality of cDNAs from each of the samples was validated by studying expression level of three housekeeping genes: *Gapdh*, *Beta-Actin* and *Hprt*. Primers used for real-time PCR were as follows: Gapdh_F: ccccaacactgagcatctcc; Gapdh_R: attatgggggtctgggatgg; ActB_F: aagtgacgttgacatccg; ActB_R: gatccacatctgctggaagg; Hprt_F: cctgtggccatctgcctagt; Hprt_R: gggacgcagcaactgacatt. Care was taken to process only single cells with consistent amplification rate of the three housekeeping genes in the same developmental stage.

The sex of each embryo was assessed by expression level analysis of *Xist* (female-specific transcript) and *Eif2s3y* (male-specific transcript) by real-time PCR. Primers used were: Eif2s3y_F: aattgccaggttattttcattttc Eif2s3y_R: agttcagtggtgcacagcaa; Xist_F: ggttctctctccagaagctaggaa and Xist_R: tggtagatggcattgtgtattatatgg.

Single cell libraries and deep-sequencing

Single-cell libraries were prepared from the 182 samples that passed QC according to the manufacturer's protocol (Illumina). Sequencing to produce single-end 50bp reads was then performed on an Illumina HiSeq 2500 instrument (Supplementary Table 1).

Quality control and filtering of raw data

Quality control was applied on raw data as previously described in (Ancelin et al, 2016)[35]. Sequencing reads characterized by at least one of the following criteria were discarded from the analysis:

1. More than 50% of low quality bases (Phred score <5).
2. More than 5% of N bases.
3. More than 80% of AT rate.
4. At least 30% (15 bases) of continuous A and/or T.

SNP calling and allele-specific origin of the transcripts

SNPs collection and strain-specific genome construction

The VCF file (mgp.v5.merged.snps_all.dbSNP142.vcf) reporting all SNP sites from 36 mouse strains based on mm10 was downloaded from the Sanger database. Using SNPsplit tool (v0.3.0)[37], these SNPs were filtered based on their quality values (FI value) and used to reconstruct the Cast genome from mm10 genome assembly.

Allele-specific alignments of RNAseq reads

To study the allele-specific gene expression, reads were processed using a pipeline adapted from Gendrel *et al,* 2014[38]. Single-end reads were first aligned to the mouse mm10 and CAST genomes using the TopHat2 software (v2.1.0)[39]. Only random best alignments with less than 2 mismatches were reported for downstream analyses. The resulting mapping files for both parental genomes were then merged for each sample, using these following rules:

1. If a read mapped at the same genomic position on the two genomes with the same number of mismatches, this read will be considered as a common read.
2. If a read is aligned with less mismatches on one genome, the best alignment will be

retained and this read will be considered as a specific read for the corresponding strain.

3. If a read is aligned with the same number of mismatches on both genomes but at different genomic positions, this read will be discarded.

Allelic imbalance in gene expression and gene classification

SNPs between *C57BL/6J* (B6) and *CAST/EiJ* (Cast) were extracted from the VCF file used to reconstruct the Cast genome. After removing common exonic SNPs between *Xist* and *Tsix* genes, 20,220,776 SNPs were retained.

The SAMtools mpileup utility (v1.1)[40] was then used to extract base-pair information at each genomic position from the merged alignment file. At each SNP position, the number of paternal and maternal allele was counted. Threshold used to call a gene informative was 5 reads mapped per single SNP with a minimum of 8 reads mapped on SNPs per gene to minimize disparity with low polymorphic gene. The allele-specific origin of the transcripts (or allelic ratio) has been measured by the total number of reads mapped on the paternal genome divided by the total number of paternal and maternal reads for each gene: allelic ratio = paternal reads / (paternal+maternal) reads.

Genes are thus classified into two categories:

1. Monoallelically expressed genes: allelic ratio value ≤ 0.15 or ≥ 0.85.
2. Biallelically expressed genes: allelic ratio value > 0.15 or < 0.85.

Estimation of gene expression levels

Given that our RNA reverse transcription only allowed sequencing up to on average 3 kilobases from the 3'UTR, half of the expressed genes are only partially covered (less than 50% of the gene size in average). To estimate transcript abundance, read counts are thus

normalized based on the amplification size of each transcript (RPRT for Reads Per Retro-Transcribed length per million mapped reads) rather than the size of each gene (RPKM).

Filtering of biased SNPs

As we observed a bias for some polymorphisms in oocytes (maternal reads only) and male cells (maternal X chromosome only), oocytes (autosomes and X-chromosomes) and males (X-chromosome) were used to address the issue. Therefore, SNPs covered by at least 5 reads and having an allelic ratio greater than 0.3 (biallelic or paternally expressed) in at least 2 of these samples were discarded. In total, 275 SNPs were filtered out, including 40 sites located on the X-chromosome.

Generation of $Xist^{pat\Delta}$ mutant embryos involved the use of a $Xist^{\Delta/Y}$ stud of mixed background (B6D2F1: *C57BL/6J* and DBA/2J, 129S1/SvlmJ and BALB/cJ). We therefore had to apply another SNP filtration to the KO samples to remove all B6 polymorphisms that could have been lost on the X chromosome due to the mixed background of the $Xist^{\Delta/Y}$ stud. To this end, all existing SNPs between B6 and DBA/2J, 129S1/SvlmJ and BALB/cJ on the X chromosome, were removed from our SNP database (34,397 SNPs, which represent 5.5% of X chromosome SNPs between B6 and Cast).

Principal component analysis, hierarchical clustering and differentially expressed genes

Count tables of gene expression were generated using the refSeq annotation and the HTSeq software[41] (v0.6.1). Only genes with a RPRT (Reads Per Retro-Transcribed length per million mapped reads) value >1 in at least 25% of the single cells of at least one developmental stage (with a minimum of 2 cells) were kept for the downstream analysis. The TMM method from the edgeR R-package (v3.14.0)[42] was first used to normalize the raw counts data. Principal component analysis (PCA) and hierarchical clustering were then used to determine how single

675 cells were clustered to the others though their gene expression profiles, depending of their
676 stage, sex and cross. PCA on normalized data was performed using FactoMineR R-package
677 (v1.33). Hierarchical clustering analysis was based on Spearman correlation distance and the
678 Ward method, using the hclust function implemented in the gplots R-package (v3.0.1).
679 Limma R-package (v3.28.4)[43] was applied to identify the differentially expressed genes
680 between 8-cell stage and blastocyst in control and *Xist*$^{pat\Delta}$ mutant females. Using the
681 Benjamini-Hochberg correction, genes with an adjusted p-value lower than α=0.05 were
682 called as differentially expressed.
683
684 **Functional enrichment analysis**
685 Down-regulated genes in *Xist*$^{pat\Delta}$ mutant female blastocysts compared to CB female
686 blastocysts were analyzed using QIAGEN's Ingenuity Pathway Analysis (IPA, QIAGEN
687 Redwood City, www.qiagen.com/ingenuity). The Functions and Diseases module has been
688 used to extract the most significantly deregulated pathways and their associated genes.
689
690 **Heatmap generation for X-chromosome allelic gene expression**
691 For BC and CB heatmaps, data from informative genes were analyzed at each developmental
692 stage only if the gene was expressed (RPRT>4) in at least 25% of single blastomeres (with a
693 minimum of 2 cells) at this particular stage and cross (Figures 2 and 4b and Supplementary
694 Figure 3). To follow the kinetics of expression, we decided to focus only on genes expressed
695 in at least 3 different stages between the 4-cell to blastocyst stages. Mean of the allelic ratio of
696 each gene is represented for the different stages. The same gene candidate list was used to
697 produce the *Xist*$^{pat\Delta}$ heatmaps (Figure 4b). A value was given only if the gene reached the
698 threshold of RPRT >4 in at least 25 % of single cells (with a minimum of 2 cells) per stage
699 and cross.

700

701 **Definition of X-linked gene silencing/escape classes**

702 We have automatically assigned X-linked genes that become strictly maternal (allelic ratio
703 ≤0.15) at the 16-cell stage or before to the "early silenced" gene class; those that become
704 maternal at the 32-cell stage to the "intermediate silenced" class (allelic ratio equals NA or
705 >0.15 at 16C and ≤0.15 at 32C) and those that are silenced only by the blastocyst stage, to the
706 "late silenced" gene class (allelic ratio equals NA or >0.15 at 16C and 32C and ≤0.15 at
707 blastocyst stage). At the blastocyst stage, X-linked genes showing a maternal bias of
708 expression (0.15<allelic ratio≤0.3) are categorized as maternally biased. A final group
709 concerns genes that escape imprinted Xp inactivation (allelic ratio >0.3 at blastocyst stage)
710 (Figure 3a). Genes escaping XCI were separated into two classes: "constitutive escapees" if
711 they were classified as escapees in both CB and BC stages and "strain-specific escapees" if
712 they were escapees in only one cross (Figure 3b and Supplementary Table 2).
713 Existence of consistency in silencing kinetics between crosses was evaluated if no more than
714 one developmental stage separated the same gene between BC and CB crosses. If the
715 consistent genes belonged to two different classes, a class for all (BC+CB) has been attributed
716 thanks to their parental ratio mean of (BC mean + CB mean) in Figure 3a and 3d.

717

718 **Dosage compensation, X:A expression ratio**

719 We measured the global X:A expression ratio in females (XX :AA ratio) and males (X :AA
720 ratio) as the level of expression of X-linked genes divided by the global level of expression of
721 the autosomal genes. Only genes with an expression value RPRT >4 were used for subsequent
722 analysis (Figures 1d and 4a). Adjustment of the number of expressed genes between X and
723 autosomes has been published to be critical for X:A expression ratio measurement[44]. We then
724 added a bootstrapping step and randomly selected, for each sample, an autosomal gene set

with the same number of expressed genes compared to the X to estimate the global X:A ratio. This step was repeated 1000 times and the X:A expression ratio was estimated as the median of the 1000 values.

Statistics section

The statistical significance has been evaluated through Dunn's Multiple Comparison Test with Benjamini-Hochberg correction and Kruskal-Wallis analysis of variance. p-values are provided in the figure legends and/or main text. Kruskal-Wallis and Post-hoc test were used to analyze non-parametric and unrelated samples.

Data availability

The Gene Expression Omnibus (GEO) accession number for the data sets reported in this paper is GSE80810.

Source data for Figure 1 (1b, 1c, 1d and 1e), Figure 3 (3a, 3b, 3c and 3d) and Figure 4 (4a and 4d) are available with the paper online.

Alll other data are available from the corresponding author upon reasonable request.

Methods-only References:

35. Ancelin, K. *et al.* Maternal LSD1 / KDM1A is an essential regulator of chromatin and transcription landscapes during zygotic genome activation. *Elife* **pii: e0885,** (2016).

36. McCloy, R. A. *et al.* Partial inhibition of Cdk1 in G2 phase overrides the SAC and decouples mitotic events. *Cell Cycle* **13,** 1400–1412 (2014).

37. Rozowsky, J. *et al.* AlleleSeq: analysis of allele-specific expression and binding in a network framework. *Mol. Syst. Biol.* **7,** 522 (2011).

38. Gendrel, A. V. *et al.* Developmental dynamics and disease potential of random monoallelic gene expression. *Dev. Cell* **28,** 366–380 (2014).

39. Kim, D. *et al.* TopHat2: accurate alignment of transcriptomes in the presence of insertions, deletions and gene fusions. *Genome Biol.* **14,** R36 (2013).

40. Krueger, F., Andrews, S. R., Krueger, F. & Andrews, S. R. SNPsplit: Allele-specific splitting of alignments between genomes with known SNP genotypes. *F1000Research* **5,** 1479 (2016).

41. Anders, S., Pyl, P. T. & Huber, W. HTSeq-A Python framework to work with high-throughput sequencing data. *Bioinformatics* **31,** 166–169 (2015).

42. Robinson, M. D., McCarthy, D. J. & Smyth, G. K. edgeR: A Bioconductor package for differential expression analysis of digital gene expression data. *Bioinformatics* **26,** 139–140 (2010).

43. Ritchie, M. E. *et al.* Limma powers differential expression analyses for RNA-sequencing and microarray studies. *Nucleic Acids Res.* **43,** e47 (2015).

44. Kharchenko, P. V, Xi, R. & Park, P. J. Evidence for dosage compensation between the X chromosome and autosomes in mammals. *Nat. Genet.* **43,** 1167–1169 (2011).

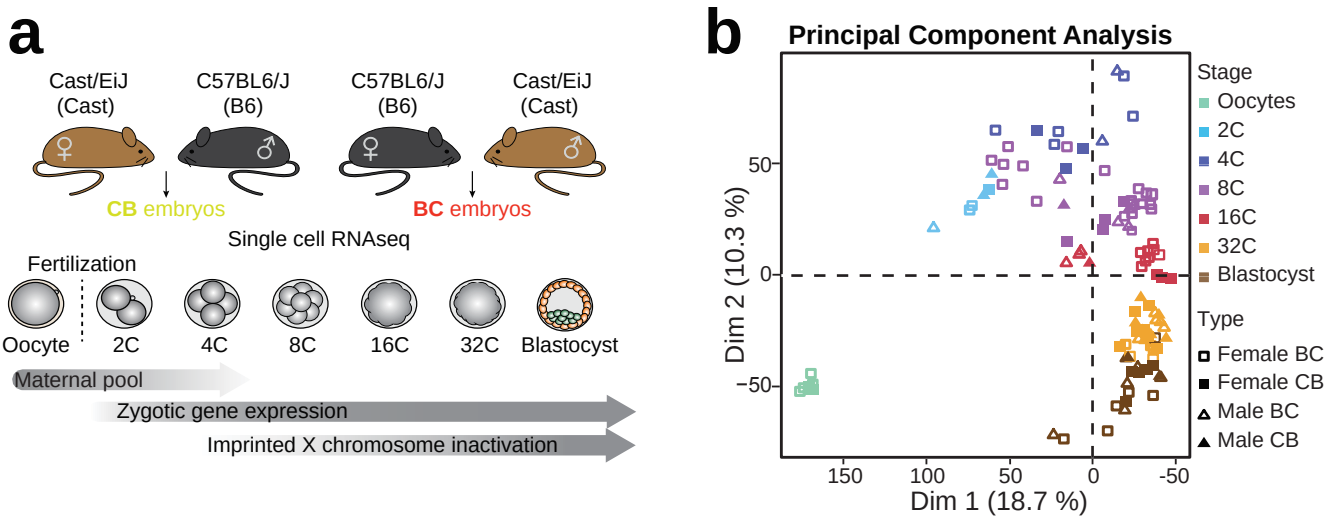
a
Cast/EiJ (Cast)
C57BL6/J (B6)
C57BL6/J (B6)
Cast/EiJ (Cast)
CB embryos
BC embryos
Single cell RNAseq
Fertilization
Oocyte
2C
4C
8C
16C
32C
Blastocyst
Maternal pool
Zygotic gene expression
Imprinted X chromosome inactivation
b
Principal Component Analysis
Dim 2 (10.3 %)
Dim 1 (18.7 %)
Stage
Oocytes
2C
4C
8C
16C
32C
Blastocyst
Type
Female BC
Female CB
Male BC
Male CB
c
Dosage compensation
Ratio X:A
2C
4C
8C
16C
32C
Blasto.
d
Allele-specific expression
Autosomes BC
X chromosomes BC
Autosomes CB
X chromosomes CB
Parental expression ratio
Paternal
Biallelic
Maternal
Blastocyst
e
XCI kinetics of candidate genes
Maternal allele
Paternal allele
Atp7a (Early)
G6pdX (Intermediate)
Atp6ap2 (Escapee)
% parental origin
Monoallelic
Biallelic
Monoallelic
Oo
Blasto.

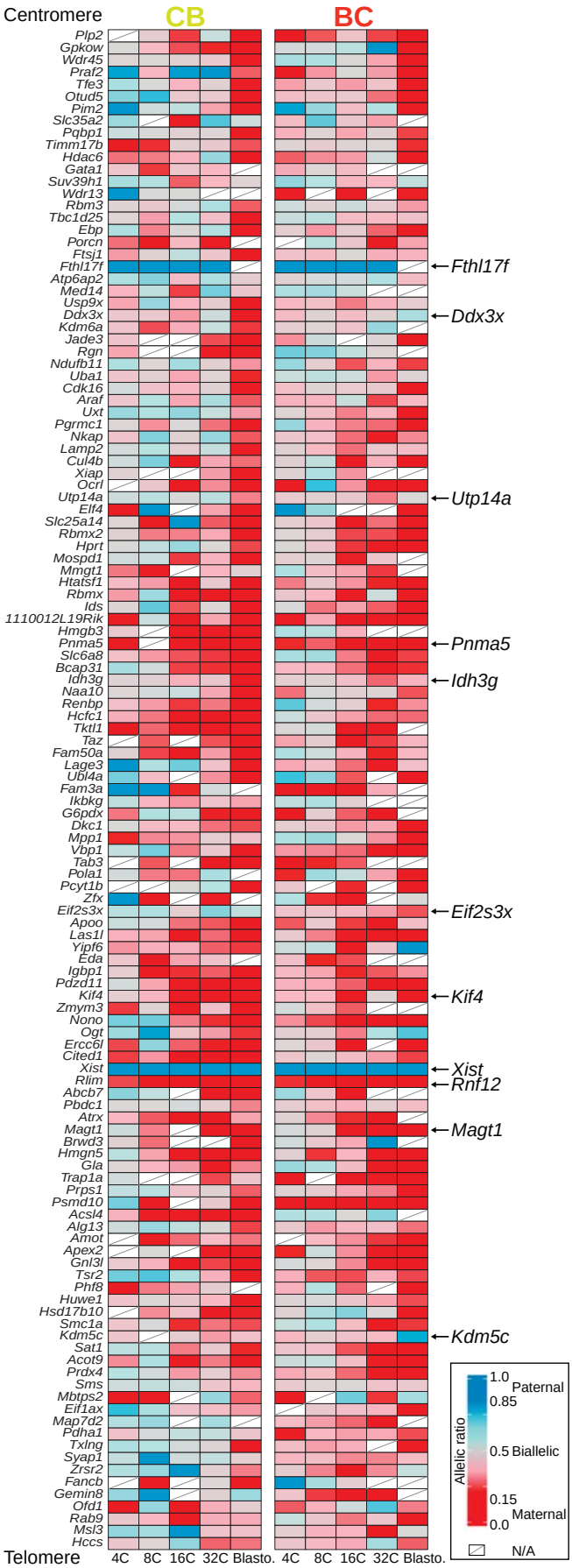
Centromere
CB
BC
Plp2
Gpkow
Wdr45
Praf2
Tfe3
Otud5
Pim2
Slc35a2
Pqbp1
Timm17b
Hdac6
Gata1
Suv39h1
Wdr13
Rbm3
Tbc1d25
Ebp
Porcn
Ftsj1
Fthl17f
Atp6ap2
Med14
Usp9x
Ddx3x
Kdm6a
Jade3
Rgn
Ndufb11
Uba1
Cdk16
Araf
Uxt
Pgrmc1
Nkap
Lamp2
Cul4b
Xiap
Ocrl
Utp14a
Elf4
Slc25a14
Rbmx2
Hprt
Mospd1
Mmgt1
Htatsf1
Rbmx
Ids
1110012L19Rik
Hmgb3
Pnma5
Slc6a8
Bcap31
Idh3g
Naa10
Renbp
Hcfc1
Tktl1
Taz
Fam50a
Lage3
Ubl4a
Fam3a
Ikbkg
G6pdx
Dkc1
Mpp1
Vbp1
Tab3
Pola1
Pcyt1b
Zfx
Eif2s3x
Apoo
Las1l
Yipf6
Eda
Igbp1
Pdzd11
Kif4
Zmym3
Nono
Ogt
Ercc6l
Cited1
Xist
Rlim
Abcb7
Pbdc1
Atrx
Magt1
Brwd3
Hmgn5
Gla
Trap1a
Prps1
Psmd10
Acsl4
Alg13
Amot
Apex2
Gnl3l
Tsr2
Phf8
Huwe1
Hsd17b10
Smc1a
Kdm5c
Sat1
Acot9
Prdx4
Sms
Mbtps2
Eif1ax
Map7d2
Pdha1
Txlng
Syap1
Zrsr2
Fancb
Gemin8
Ofd1
Rab9
Msl3
Hccs
Fthl17f
Ddx3x
Utp14a
Pnma5
Idh3g
Eif2s3x
Kif4
Xist
Rnf12
Magt1
Kdm5c
Telomere
4C 8C 16C 32C Blasto. 4C 8C 16C 32C Blasto.
Allelic ratio
1.0
0.85
Paternal
0.5 Biallelic
0.15
0.0
Maternal
N/A

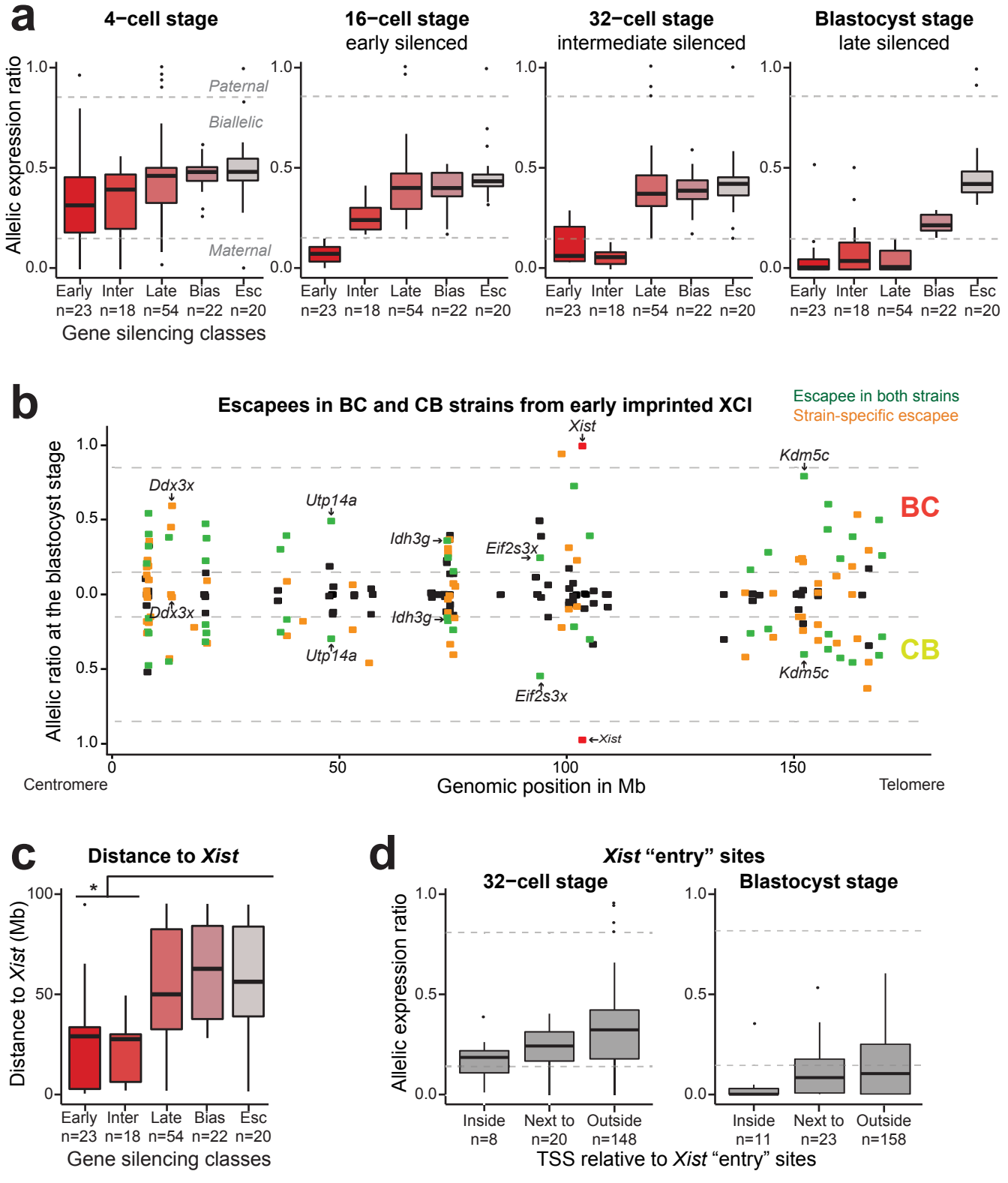
a
4−cell stage
16−cell stage
early silenced
32−cell stage
intermediate silenced
Blastocyst stage
late silenced
Allelic expression ratio
Paternal
Biallelic
Maternal
1.0
0.5
0.0
Early n=23
Inter n=18
Late n=54
Bias n=22
Esc n=20
Gene silencing classes
b
Escapees in BC and CB strains from early imprinted XCI
Escapee in both strains
Strain-specific escapee
Allelic ratio at the blastocyst stage
Xist
Kdm5c
Ddx3x
Utp14a
Idh3g
Eif2s3x
BC
CB
←Xist
0
50
100
150
Centromere
Genomic position in Mb
Telomere
c
Distance to Xist
Distance to Xist (Mb)
100
50
0
*
Early n=23
Inter n=18
Late n=54
Bias n=22
Esc n=20
Gene silencing classes
d
Xist "entry" sites
32−cell stage
Blastocyst stage
Allelic expression ratio
1.0
0.5
0.0
Inside n=8
Next to n=20
Outside n=148
Inside n=11
Next to n=23
Outside n=158
TSS relative to Xist "entry" sites

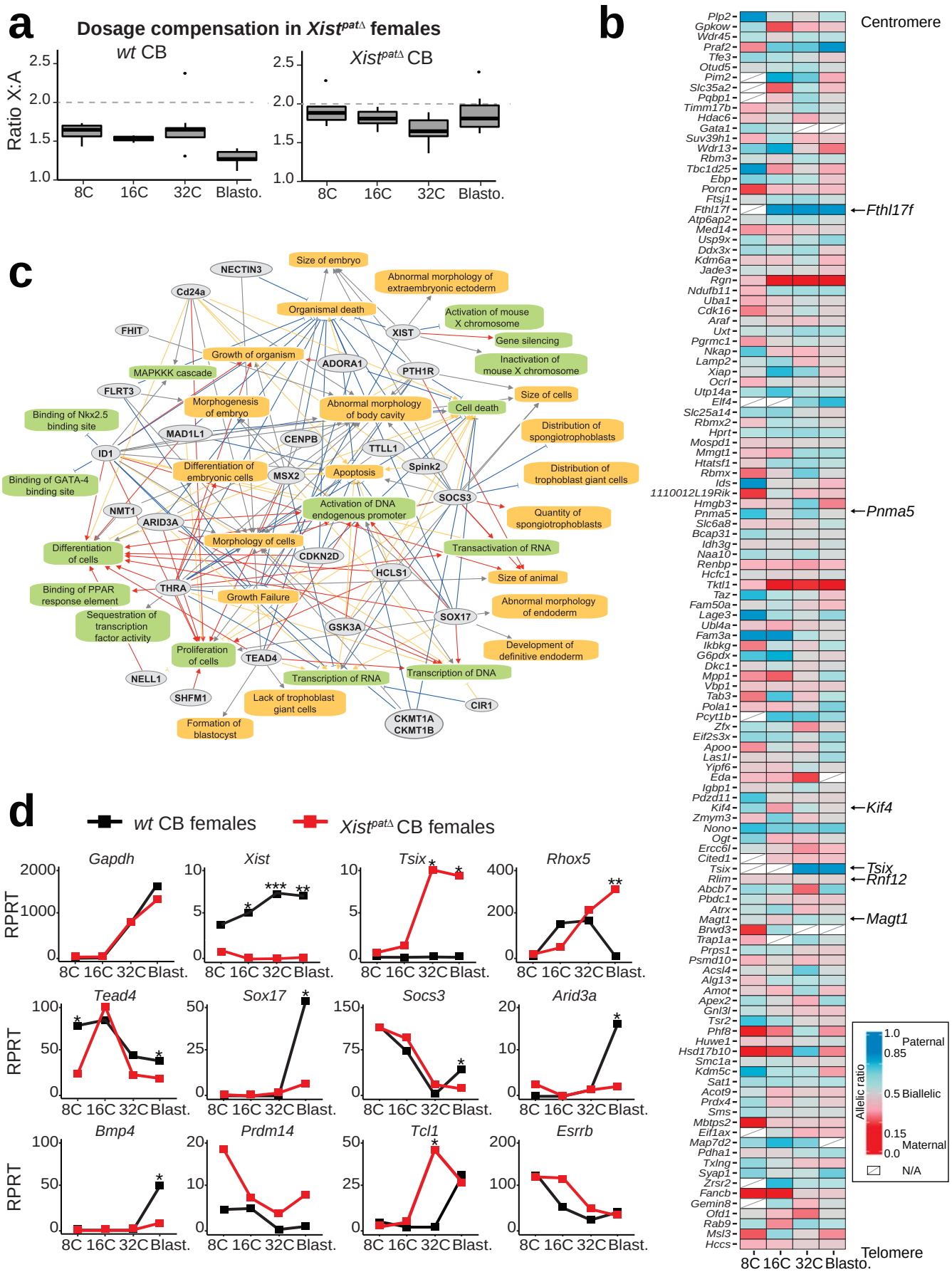
a
Dosage compensation in Xist^patΔ females
wt CB
Xist^patΔ CB
Ratio X:A
2.5
2.0
1.5
1.0
8C
16C
32C
Blasto.
b
Centromere
Telomere
Fthl17f
Pnma5
Kif4
Tsix
Rnf12
Magt1
Allelic ratio
1.0
Paternal
0.85
0.5 Biallelic
0.15
0.0
Maternal
N/A
c
NECTIN3
Size of embryo
Cd24a
Abnormal morphology of extraembryonic ectoderm
Organismal death
Activation of mouse X chromosome
FHIT
XIST
Gene silencing
Growth of organism
ADORA1
Inactivation of mouse X chromosome
MAPKKK cascade
PTH1R
FLRT3
Morphogenesis of embryo
Abnormal morphology of body cavity
Cell death
Size of cells
Binding of Nkx2.5 binding site
MAD1L1
CENPB
Distribution of spongiotrophoblasts
ID1
TTLL1
Differentiation of embryonic cells
MSX2
Apoptosis
Spink2
Distribution of trophoblast giant cells
Binding of GATA-4 binding site
SOCS3
NMT1
Activation of DNA endogenous promoter
Quantity of spongiotrophoblasts
ARID3A
Differentiation of cells
Morphology of cells
CDKN2D
Transactivation of RNA
HCLS1
Size of animal
Binding of PPAR response element
THRA
Growth Failure
Abnormal morphology of endoderm
Sequestration of transcription factor activity
SOX17
GSK3A
Development of definitive endoderm
Proliferation of cells
TEAD4
NELL1
Transcription of RNA
Transcription of DNA
SHFM1
Lack of trophoblast giant cells
CIR1
Formation of blastocyst
CKMT1A
CKMT1B
d
wt CB females
Xist^patΔ CB females
RPRT
Gapdh
Xist
Tsix
Rhox5
Tead4
Sox17
Socs3
Arid3a
Bmp4
Prdm14
Tcl1
Esrrb
8C 16C 32C Blast.

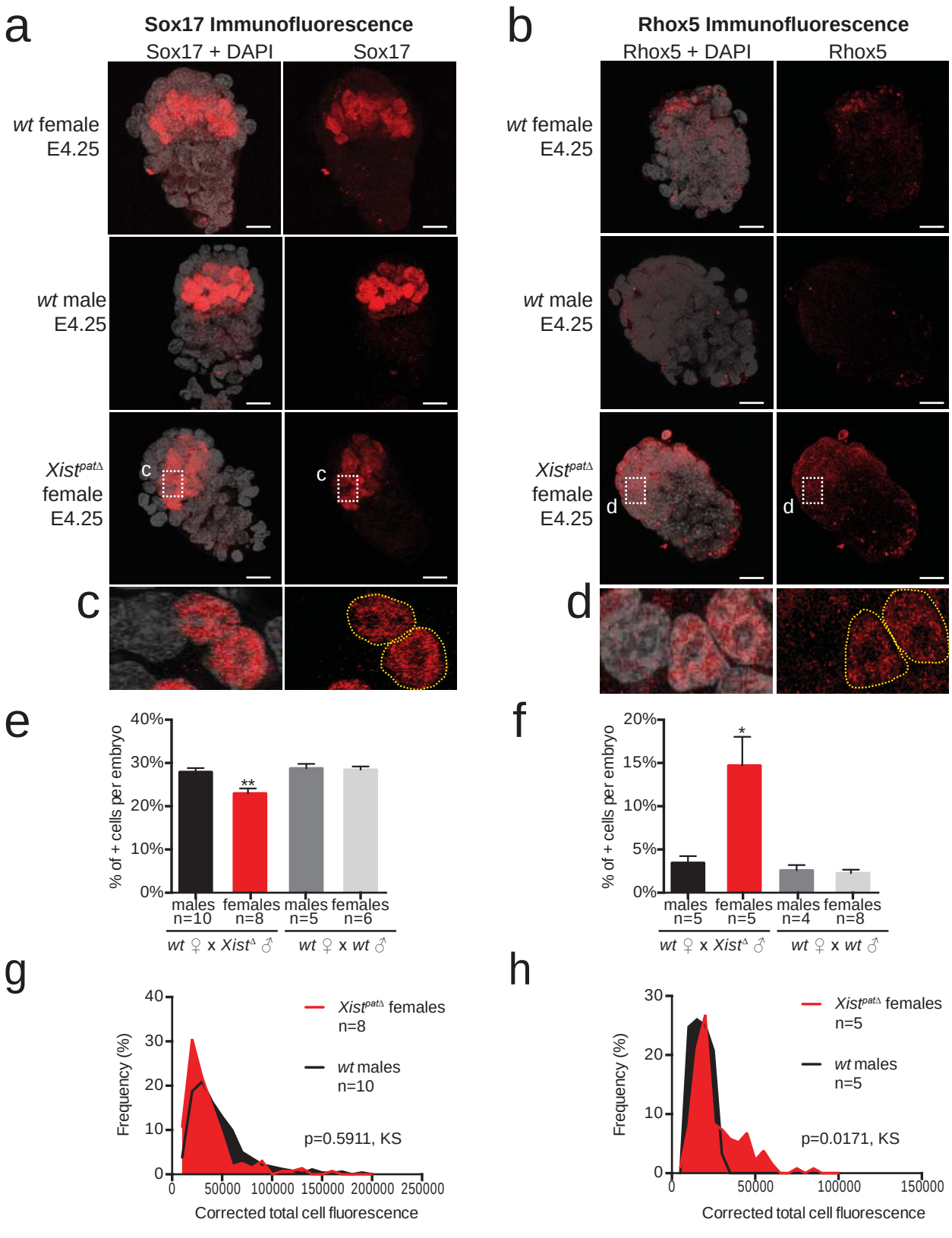
a
Sox17 Immunofluorescence
Sox17 + DAPI
Sox17
wt female E4.25
wt male E4.25
Xist^patΔ female E4.25
c
b
Rhox5 Immunofluorescence
Rhox5 + DAPI
Rhox5
wt female E4.25
wt male E4.25
Xist^patΔ female E4.25
d
e
% of + cells per embryo
40%
30%
20%
10%
0%
**
males n=10
females n=8
males n=5
females n=6
wt ♀ x Xist^Δ ♂
wt ♀ x wt ♂
f
% of + cells per embryo
20%
15%
10%
5%
0%
*
males n=5
females n=5
males n=4
females n=8
wt ♀ x Xist^Δ ♂
wt ♀ x wt ♂
g
Frequency (%)
40
30
20
10
0
Xist^patΔ females n=8
wt males n=10
p=0.5911, KS
0
50000
100000
150000
200000
250000
Corrected total cell fluorescence
h
Frequency (%)
30
20
10
0
Xist^patΔ females n=5
wt males n=5
p=0.0171, KS
0
50000
100000
150000
Corrected total cell fluorescence

Supplementary Table 1: Silencing classes for informative and well-expressed X-linked genes in BC and CB crosses.

Silencing classes for the 173 informative and well-expressed X-linked genes in BC and/or CB crosses.

All genes		
Genes	BC	CB
1110012L19Rik	Early	Early
1810030O07Rik	NA	Esc
A230072C01Rik	NA	Late
Abcb7	Early	Late
Abcd1	Esc	NA
Acot9	Late	Early
Acsl4	Late	Inter
Alg13	Bias	Bias
Amot	Late	Bias
Apex2	Inter	Late
Apoo	Inter	Late
Araf	Esc	Bias
Atp11c	Inter	NA
Atp6ap2	Esc	Esc
Atp7a	Early	NA
Atrx	Inter	Early
BC065397	NA	Late
Bcap31	Inter	Late
Bex1	NA	Late
Bhlhb9	NA	Late
Brcc3	NA	Inter
Brwd3	Late	Late
Ccdc22	Late	NA
Cdk16	Late	Late
Cenpi	Late	NA
Cetn2	Late	NA
Cited1	Bias	Inter
Ctps2	Bias	NA
Cul4b	Late	Bias
Ddx3x	Esc	Late
Dkc1	Bias	Bias
Dlg3	Early	NA
Ebp	Late	Bias
Eda	Late	Late
Eif1ax	Late	Esc
Eif2s3x	Bias	Esc
Elf4	Late	Late
Emd	Early	NA
Eras	Early	NA
Ercc6l	Early	Late
Fam3a	Early	Late
Fam50a	Esc	Early
Fancb	Late	Late
Flna	Early	NA
Fmr1	Late	NA
Fmr1nb	Early	NA
Fthl17f	Late	Late
Ftsj1	Esc	Late
Fundc1	Esc	NA
G6pdx	Inter	Late
Gata1	Late	Late
Gdi1	Esc	NA
Gemin8	Early	Esc
Gla	Inter	Inter
Gm6880	Early	NA
Gnl3l	Inter	Early
Gpc4	Early	NA
Gpkow	Late	Late
Gspt2	Inter	NA
Haus7	Early	NA
Hccs	Bias	Bias
Hcfc1	Bias	Early
Hdac6	Late	Late
Hmgb3	Late	Early
Hmgn5	Inter	Early
Hprt	Inter	Bias
Hsd17b10	Late	Inter
Htatsf1	Late	Late
Huwe1	Bias	Late
Idh3g	Esc	Bias
Ids	Late	Late
Igbp1	Esc	Late
Ikbkg	Late	Esc
Il2rg	Late	NA
Irak1	Inter	NA
Jade3	Late	Late
Kdm5c	Esc	Esc
Kdm6a	Late	Bias
Kif4	Early	Early
Klf8	Inter	NA
Klhl15	Late	NA
Lage3	Inter	Late
Lamp2	Esc	Bias
Las1l	Inter	Early
Magea5	Late	NA
Maged1	Early	NA
Magt1	Early	Inter
Map7d2	Inter	Late
Mbtps2	Esc	Bias

All genes		
Genes	BC	CB
Mdrl	Late	NA
Med12	Early	NA
Med14	Late	Esc
Mmgt1	Late	Esc
Mospd1	Late	Late
Mpp1	Late	Esc
Msl3	Esc	Esc
Mtm1	Early	NA
Naa10	Bias	Bias
Ndufb11	Bias	Esc
Nkap	Esc	Bias
Nono	Inter	Late
Nsdhl	NA	Inter
Ocrl	Inter	Early
Ofd1	Bias	Early
Ogt	Esc	Bias
Otud5	Bias	Late
Pbdc1	Esc	Esc
Pcyt1b	Late	Late
Pdha1	Bias	Esc
Pdzd11	Inter	Inter
Pgk1	Inter	NA
Pgrmc1	Late	Late
Phf6	Late	NA
Phf8	Late	Late
Pim2	Late	Late
Plp2	Late	Late
Pls3	Inter	NA
Pnma5	Early	Early
Pola1	Late	Late
Porcn	Inter	Late
Pqbp1	Bias	Late
Praf2	Late	Bias
Prdx4	Inter	Esc
Prps1	Bias	Bias
Psmd10	Early	Late
Rab9	Bias	Early
Rbm3	Esc	Bias
Rbmx	Early	Early
Rbmx2	Late	Late
Renbp	Esc	Late
Rgn	Late	Late
Ribc1	Early	NA
Rlim	Early	Early
Rpgr	NA	Late
Rpl10	Inter	NA
Sat1	Inter	Bias
Slc25a14	Early	Late
Slc25a53	Early	NA
Slc35a2	Late	Early
Slc6a8	Inter	Late
Smc1a	Inter	Bias
Sms	Esc	Esc
Snx12	Early	NA
Suv39h1	Esc	Esc
Syap1	Esc	Esc
Tab3	Late	Inter
Taf1	Late	NA
Taz	Early	Late
Tbc1d25	Esc	Bias
Tfe3	Late	Bias
Timm17b	Bias	Bias
Tktl1	Early	Early
Tmem164	Late	NA
Tmem185a	Late	NA
Trap1a	Early	Esc
Tsr2	Bias	Late
Txlng	Bias	Late
Uba1	Esc	Bias
Ubl4a	Late	Late
Usp9x	Esc	Late
Utp14a	Esc	Bias
Uxt	Late	Esc
Vbp1	Inter	Bias
Vma21	NA	Late
Wdr13	Bias	Late
Wdr45	Late	Bias
Wnk3	Late	NA
Xiap	Late	Bias
Xist	Esc	Esc
Yipf6	Early	Bias
Zfx	Early	Late
Zmym3	Late	Early
Zrsr2	Early	Bias

Consistent genes			
Genes	BC	CB	All
1110012L19Rik	Early	Early	Early
Acsl4	Late	Inter	Late
Alg13	Bias	Bias	Bias
Amot	Late	Bias	Late
Apex2	Inter	Late	Inter
Apoo	Inter	Late	Inter
Araf	Esc	Bias	Esc
Atp6ap2	Esc	Esc	Esc
Atrx	Inter	Early	Inter
Bcap31	Inter	Late	Bias
Brwd3	Late	Late	Late
Cdk16	Late	Late	Late
Cul4b	Late	Bias	Bias
Dkc1	Bias	Bias	Bias
Ebp	Late	Bias	Late
Eda	Late	Late	Late
Eif2s3x	Bias	Esc	Esc
Elf4	Late	Late	Late
Fancb	Late	Late	Late
Fthl17f	Late	Late	Late
G6pdx	Inter	Late	Inter
Gata1	Late	Late	Late
Gla	Inter	Inter	Inter
Gnl3l	Inter	Early	Late
Gpkow	Late	Late	Late
Hccs	Bias	Bias	Bias
Hdac6	Late	Late	Late
Hmgn5	Inter	Early	Inter
Hsd17b10	Late	Inter	Late
Htatsf1	Late	Late	Late
Huwe1	Bias	Late	Bias
Idh3g	Esc	Bias	Bias
Ids	Late	Late	Late
Jade3	Late	Late	Late
Kdm5c	Esc	Esc	Esc
Kdm6a	Late	Bias	Bias
Kif4	Early	Early	Early
Lage3	Inter	Late	Bias
Lamp2	Esc	Bias	Bias
Las1l	Inter	Early	Early
Magt1	Early	Inter	Early
Map7d2	Inter	Late	Late
Mbtps2	Esc	Bias	Esc
Mospd1	Late	Late	Late
Msl3	Esc	Esc	Esc
Naa10	Bias	Bias	Bias
Ndufb11	Bias	Esc	Bias
Nkap	Esc	Bias	Bias
Nono	Inter	Late	Inter
Ocrl	Inter	Early	Late
Ogt	Esc	Bias	Esc
Otud5	Bias	Late	Late
Pbdc1	Esc	Esc	Esc
Pcyt1b	Late	Late	Late
Pdha1	Bias	Esc	Esc
Pdzd11	Inter	Inter	Inter
Pgrmc1	Late	Late	Late
Phf8	Late	Late	Late
Pim2	Late	Late	Late
Plp2	Late	Late	Late
Pnma5	Early	Early	Early
Pola1	Late	Late	Late
Porcn	Inter	Late	Esc
Pqbp1	Bias	Late	Late
Praf2	Late	Bias	Late
Prps1	Bias	Bias	Bias
Rbm3	Esc	Bias	Bias
Rbmx	Early	Early	Early
Rbmx2	Late	Late	Late
Rgn	Late	Late	Late
Rlim	Early	Early	Early
Slc6a8	Inter	Late	Late
Sms	Esc	Esc	Esc
Suv39h1	Esc	Esc	Esc
Syap1	Esc	Esc	Esc
Tab3	Late	Inter	Inter
Tbc1d25	Esc	Bias	Bias
Tfe3	Late	Bias	Late
Timm17b	Bias	Bias	Bias
Tktl1	Early	Early	Early
Tsr2	Bias	Late	Bias
Txlng	Bias	Late	Late
Uba1	Esc	Bias	Esc
Ubl4a	Late	Late	Late
Utp14a	Esc	Bias	Esc
Wdr13	Bias	Late	Bias
Wdr45	Late	Bias	Bias
Xiap	Late	Bias	Bias
Xist	Esc	Esc	Esc

Supplementary Table 2: Summary of escapees and their status in other studies

Information for escapees is provided for CB and BC crosses. Status of each escapee gene has been evaluated in other studies using hybrid cell lines or tissues (Calabrese *et al*, *Cell*, 2012; Berletch *et al*, *PLOS Genet*, 2015; Marks *et al*, *Genome Biol*, 2015; Gendrel *et al*, *Dev Cell*, 2014)

Gene Symbol	BC embryos	CB embryos	TSC (Calabrese et al)	Brain (Berletch et al)	Spleen (Berletch et al)	Ovary (Berletch et al)	Patski (Berletch et al)	NPC* (Marks et al)	NPC** (Gendrel et al)
1810030O07Rik	-	**yes**	no			**yes**	**yes**	yes (1/3)	**yes (4/4)**
Abcd1	**yes**	no	no					-	yes (2/4)
Alg13	biased	biased	-			**yes**		no	yes (1/4)
Amot	no	biased	no				**yes**	no	no
Araf	**yes**	biased	no					yes (1/3)	**yes (4/4)**
Atp6ap2	**yes**	**yes**	-					no	yes (2/4)
Cited	biased	no	no					-	no
Ctps2	biased	-	no				**yes**	no	yes (3/4)
Cul4b	no	biased	no					-	-
Ddx3x	**yes**	no	no	**yes**	**yes**	**yes**	**yes**	**yes (3/3)**	**yes (4/4)**
Dkc1	biased	biased	no					**yes**	no
Ebp	no	biased	no				**yes**	yes (1/3)	yes (2/4)
Eif1ax	no	**yes**	-					no	yes (2/4)
Eif2s3x	biased	**yes**	**yes**	**yes**	**yes**	**yes**	**yes**	-	**yes (4/4)**
Fam50a	**yes**	no	-				**yes**	-	yes (2/4)
Ftsj1	**yes**	no	no					yes (2/3)	**yes (4/4)**
Fundc1	**yes**	-	no					no	yes (2/4)
Gdi1	**yes**	-	no	**yes**				no	yes (2/4)
Gemin8	no	**yes**	no					-	**yes (4/4)**
Hccs	biased	biased	no					no	yes (3/4)
Hcfc1	biased	no	no					yes (2/3)	**yes (4/4)**
Hprt	no	biased	no					no	no
Huwe1	biased	no	no			**yes**		no	yes (3/4)
Idh3g	**yes**	biased	no			**yes**	**yes**	no	yes (2/4)
Igbp1	**yes**	no	no					no	yes (3/4)
Ikbkg	no	**yes**	no				**yes**	no	yes (1/4)
Kdm5c	**yes**	**yes**	**yes**	**yes**	**yes**	**yes**	**yes**	**yes (3/3)**	**yes (4/4)**
Kdm6a	no	biased	**yes**	**yes**	**yes**	**yes**	**yes**	**yes (3/3)**	**yes (4/4)**
Lamp2	**yes**	biased	no			**yes**	**yes**	no	yes (1/4)
Mbtps2	**yes**	biased	no					no	yes (1/4)
Med14	no	**yes**	no					yes (2/3)	**yes (4/4)**
Mmgt1	no	**yes**	-			**yes**		-	yes (2/4)
Mpp1	no	**yes**	no					no	no
Msl3	**yes**	**yes**	no					no	yes (2/4)
Naa10	biased	biased	-					-	yes (2/4)
Ndufb11	biased	**yes**	no					yes (1/3)	**yes (4/4)**
Nkap	**yes**	biased	**yes CB only**					yes (2/3)***	yes (3/4)
Ofd1	biased	no	no				**yes**	yes (2/3)	yes (3/4)
Ogt	**yes**	biased	**yes**					no	**yes (4/4)**
Pbdc1	**yes**	**yes**	-		**yes**	**yes**	**yes**	-	**yes (4/4)**
Pdha1	biased	**yes**	no			**yes**		no	no
Pqbp1	biased	no	**yes BC only**					no	yes (3/4)
Praf2	no	biased	**-**					-	yes (3/4)
Prdx4	no	**yes**	no					no	no
Prps1	biased	biased	no					no	no
Rab9	biased	no	no					no	yes (3/4)
Rbm3	**yes**	biased	no					yes (1/3)	yes (2/4)
Renbp	**yes**	no	no					no	yes (2/4)
Sat1	no	biased	**no**					no	no
Smc1a	no	biased	**no**					no	yes (3/4)
Sms	**yes**	**yes**	no					no	no
Suv39h1	**yes**	**yes**	**yes BC only**					no	**yes (4/4)**
Syap1	**yes**	**yes**	**yes CB only**					no	yes (3/4)
Tbc1d25	**yes**	biased	no					yes (1/3)	yes (2/4)
Tfe3	no	biased	no					-	-
Timm17b	biased	biased	no					yes (2/3)	yes (3/4)
Trap1a	no	**yes**	no					-	-
Tsr2	biased	no	no					no	no
Txlng	biased	no	no					yes (1/3)	yes (3/4)
Uba1a	**yes**	biased	-			**yes**		yes (2/3)	**yes (4/4)**
Usp9x	**yes**	no	no			**yes**		yes (2/3)	yes (3/4)
Utp14a	**yes**	biased	**yes**		**yes**	**yes**		**yes (3/3)**	**yes (4/4)**
Uxt	no	**yes**	no					-	yes (1/4)
Vbp1	no	biased	no				**yes**	yes (2/3)	yes (2/4)
Wdr13	biased	no	no				**yes**	yes (1/3)	yes (3/4)
Wdr45	no	biased	no					yes (1/3)	yes (3/4)
Xiap	no	biased	-					no	no
Xist	**yes**	**yes**	**yes**	**yes**	**yes**	**yes**	**yes**	**yes (3/3)**	**yes (4/4)**
Yipf6	no	**yes**	**yes**				**yes**	no	yes (1/4)
Zrsr2	no	biased	**yes**					yes (1/3)	yes (3/4)

* NPC data are derived from 3 independant clones. Information of escape for each clone is provided in brackets.

** NPC data are derived from 4 independant clones. Information of escape for each clone is provided in brackets.

*** *Nkap* escapes from Cast Xi and from 129 Xi.

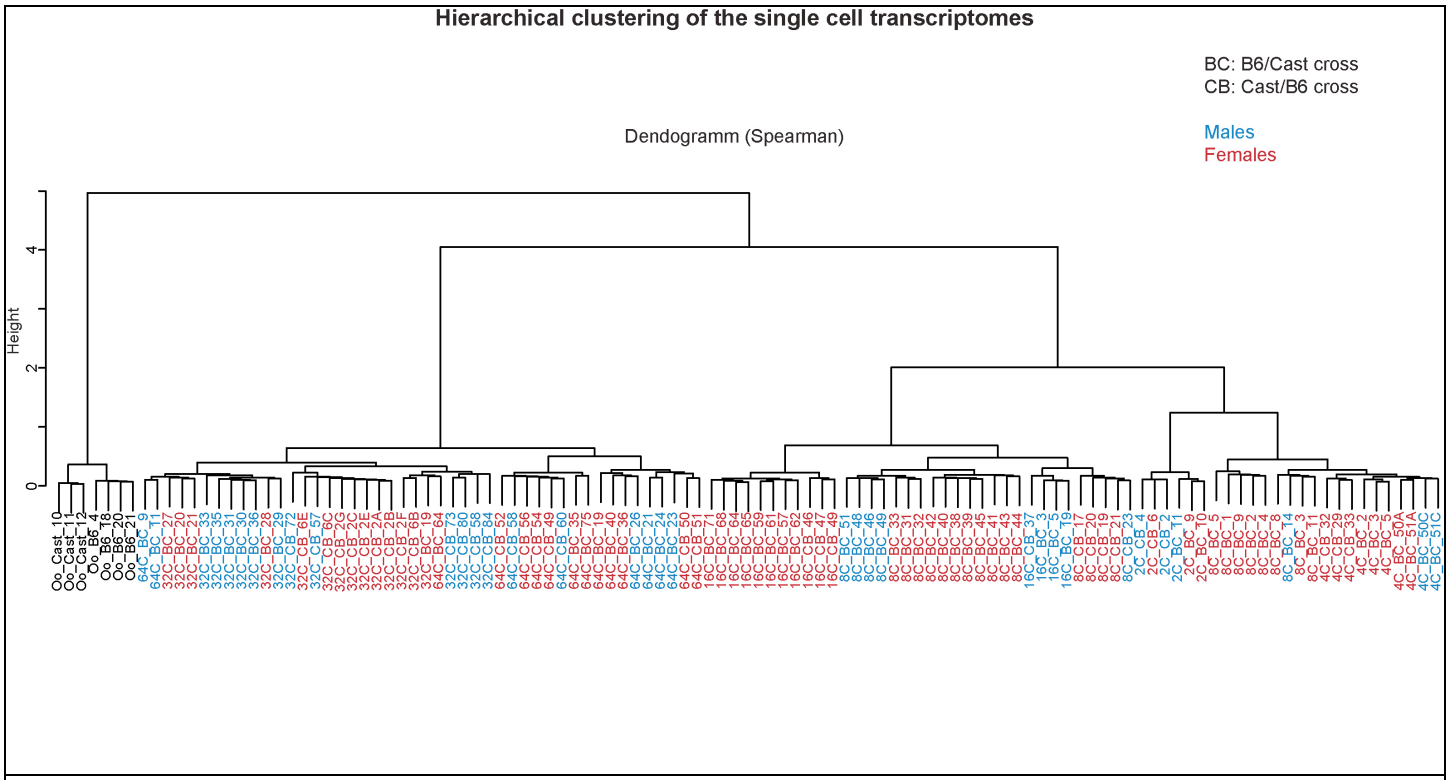

Supplementary Figure 1

Hierarchical clustering of scRNAseq

Hierarchical clustering of single cell transcriptomes, based on Spearman's correlation. Cells were clustered by developmental stage, then by cross (BC or CB), and finally according to their sex. ScRNAseq samples called 64C are related to the early blastocyst stage. n=184 single cell samples

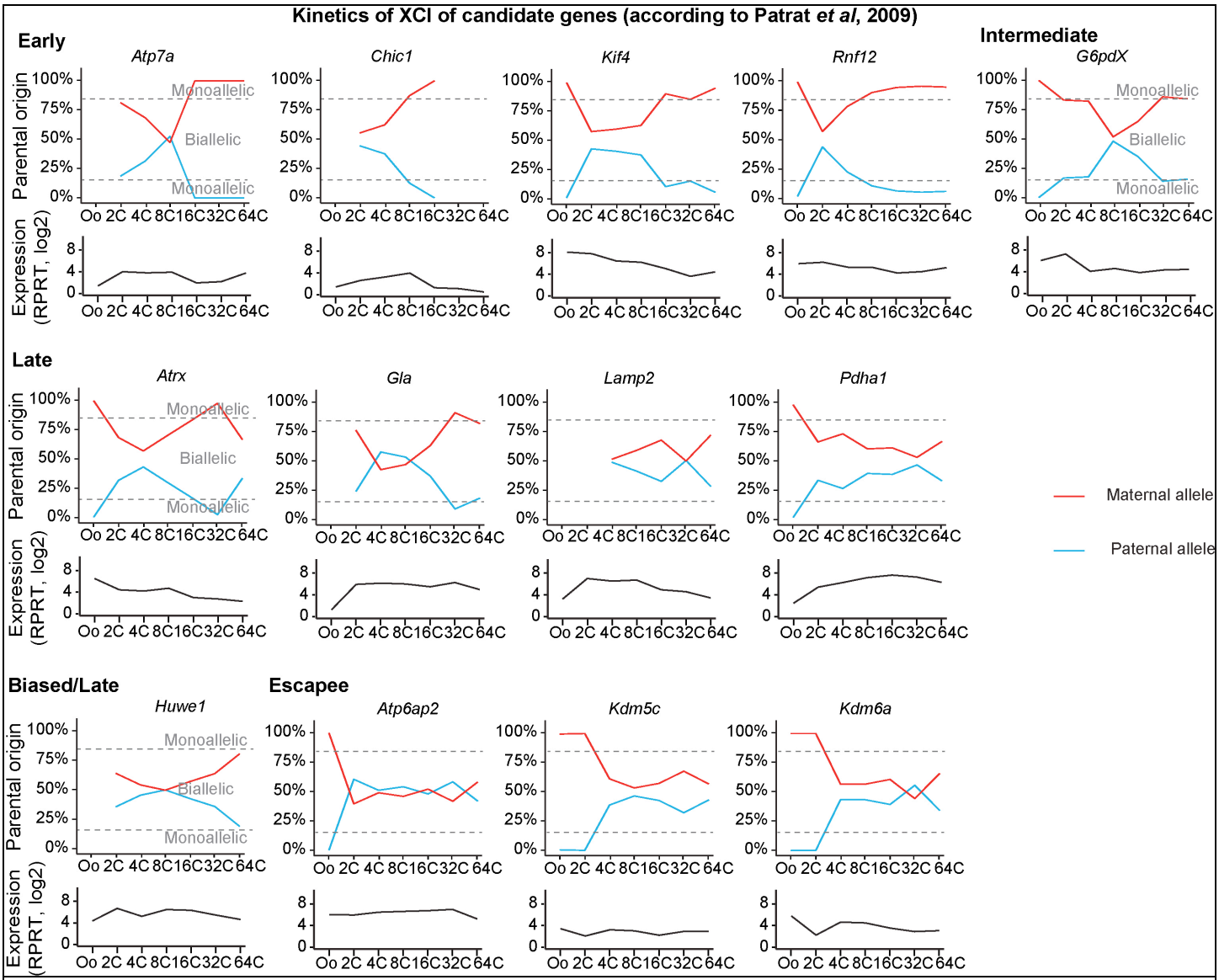

Supplementary Figure 2

Single cell RNA sequencing data corroborate RNA-FISH based silencing of kinetics.

Candidate X-linked gene silencing kinetics (scRNA-seq) is compared to previous kinetics studied by RNA-FISH in Patrat *et al*, 2009[14]. Mean of maternal and paternal reads are respectively represented as red or blue lines. Percentage of parental origin transcript (top panel) and level of expression in RPRT (bottom panel) of each gene are represented between oocytes and blastocysts.

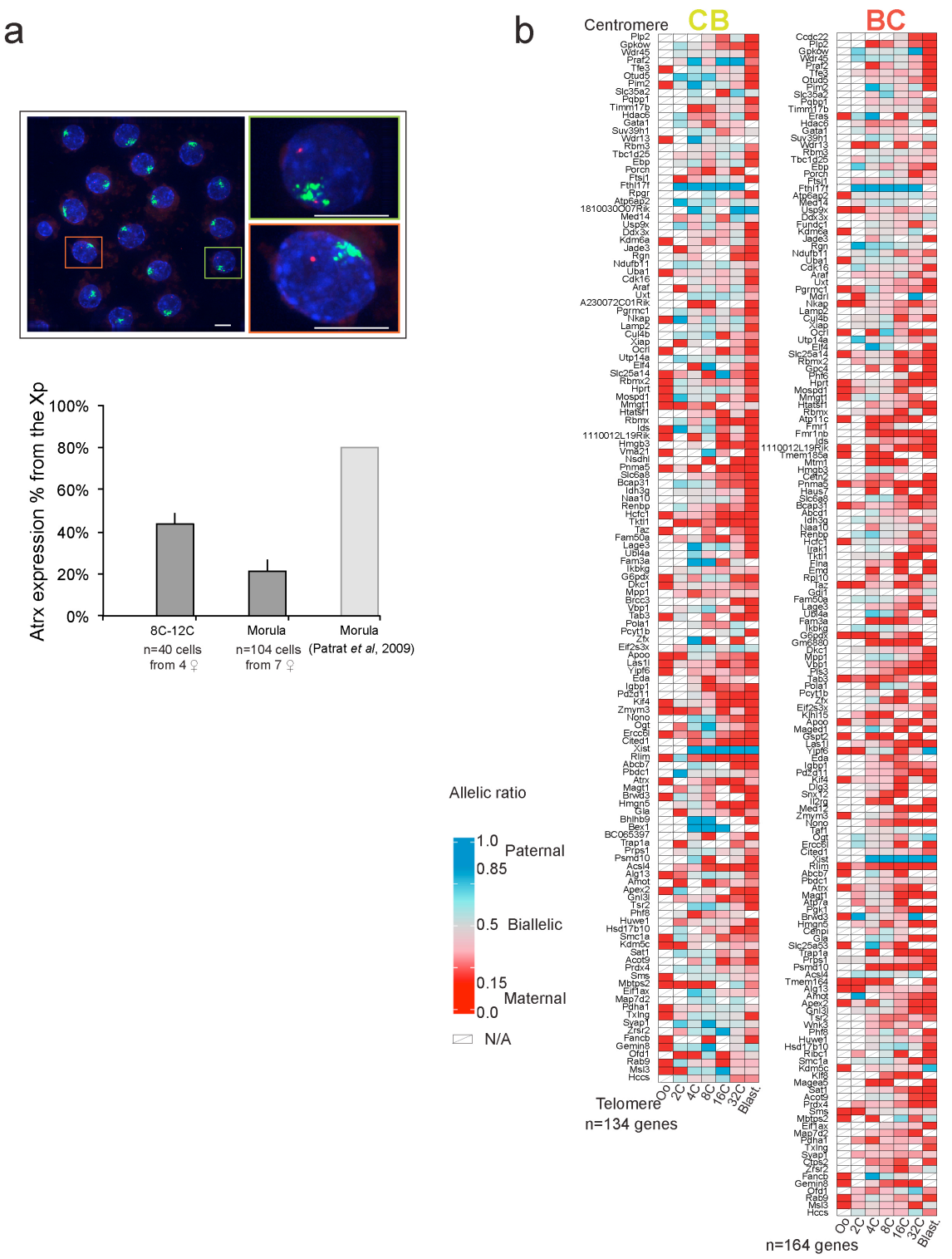

Supplementary Figure 3

Gene validation by RNA-FISH and chromosome-wide representation of parental expression ratio.

(a) Nascent RNA FISH using probes recognizing *Xist* (signal in green) and *Atrx* (signal in red) RNAs on a 16C female embryo. DAPI is

in blue. Right pictures are enhanced pictures of two individual blastomeres. Percentage of nuclei showing pinpoints of nascent transcripts by RNA FISH from Xp and Xm has been assessed and summarized as the median + s.e.m. under the picture. Normalization of the primary transcript detection frequency obtained for the paternal (*Xist* RNA-associated) allele in female embryos was achieved thanks to the detection frequency obtained for the maternal allele in male embryos at the same stage. Number of embryos and single cell processed are indicated under each genotype. Scale bars represent 10µm.

(b) Heatmaps are shown representing the mean of allele-specific expression of X-linked genes, from Oocytes to blastocysts in CB and BC crosses. Strictly maternally expressed genes (allelic ratio ≤0.15) are represented in red and strictly paternally expressed genes (allelic ratio ≥0.85) in blue. Color gradients are used in between and genes have been ordered by genomic position. Oocytes and 2C stage data, as well as strain-specific gene expression data, have been included, in addition to the heatmaps for the stages shown in Figure 2.

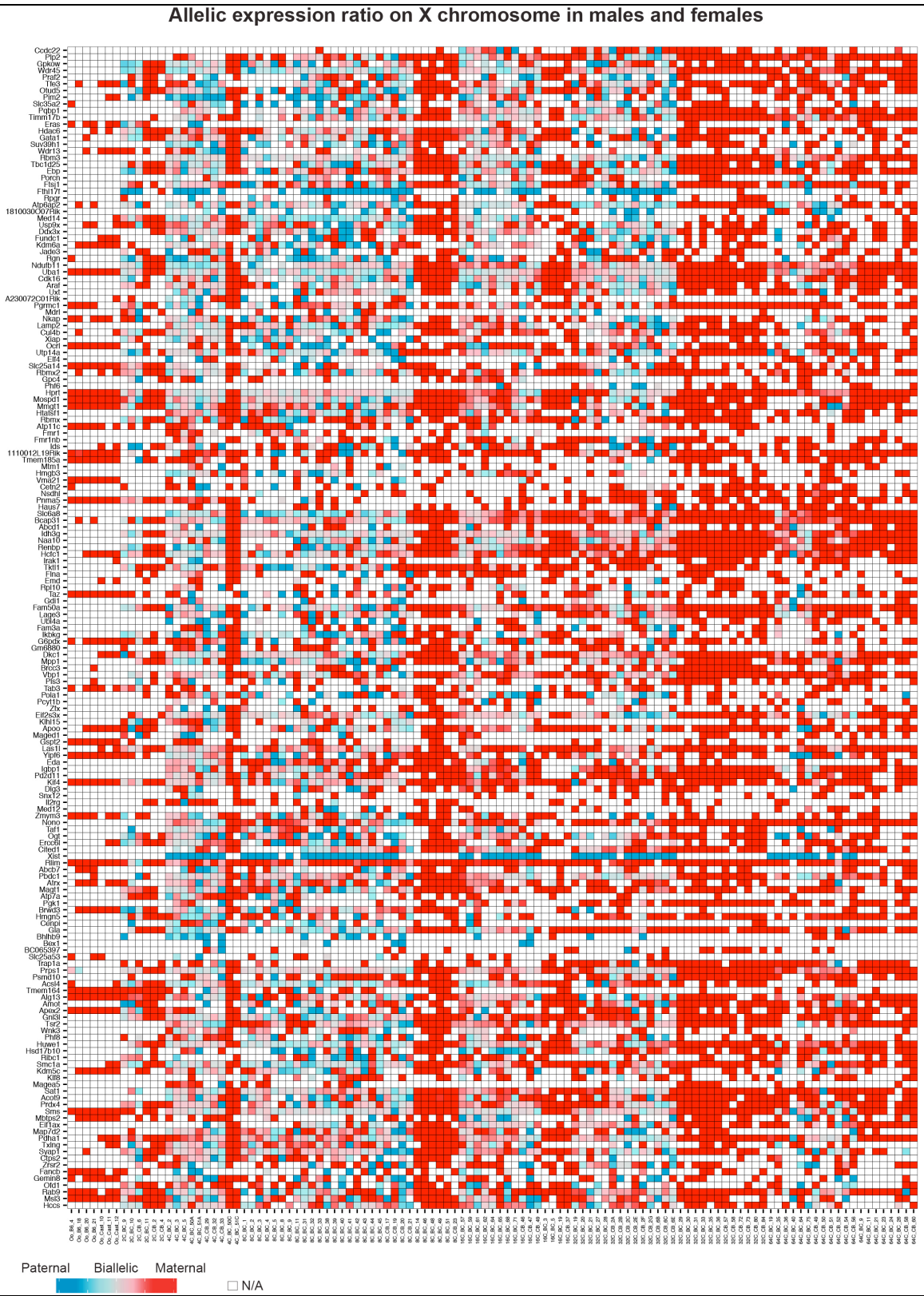

Supplementary Figure 4

Complete single cell information of X-linked gene expression in pre-implantation development

Heatmap representing the full allele-specific expression data set of informative and well-expressed X-linked genes in each single cell, from oocytes to blastocysts, in male and female embryos derived from BC and CB crosses. Strictly maternally expressed genes (allelic ratio ≤0.15) are represented in red and strictly paternally expressed genes (allelic ratio ≥0.85) in blue. Color gradients are used in between and genes have been ordered by genomic position. Genes expressed in one or both crosses have been included to the single cell heatmap. n=173 genes.

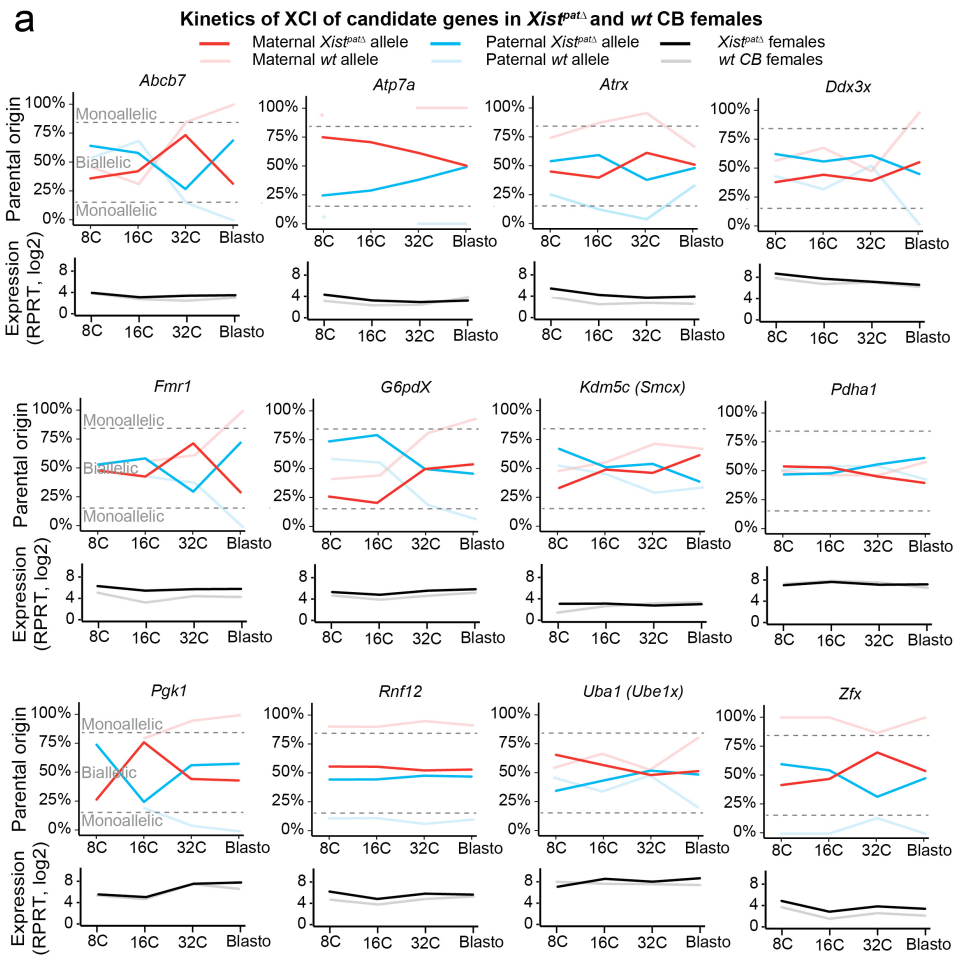

b **Total differentially expressed genes in *Xist*^{patΔ} CB females**

Developmental stages	DE genes from the X chromosome				DE genes from the autosomes			
	Total Upregulated		Total Downregulated		Total Upregulated		Total Downregulated	
	%	n	%	n	%	n	%	n
8-cell	5.0%	27	1.9%	14	95.0%	514	98.1%	541
16-cell	11.6%	15	1.0%	1	88.4%	114	99.0%	129
32-cell	4.7%	29	2.3%	12	95.3%	591	97.7%	620
Blastocyst	29.6%	16	3.6%	2	70.4	38	96.4%	54

Supplementary Figure 5

Absence of X-chromosome inactivation in absence of Xist.

(a) Each plot represents a candidate X-linked gene that was previously studied in Kalantry *et al*, 2009[6]. Allele-specific expression ratio of each gene represents the number of reads mapped on paternal genome divided by the total number of paternal and maternal reads. Mean of maternal and paternal reads are respectively represented as a red or a blue line. Percentage of parental origin transcript (top panel) and level of expression in RPRT (bottom panel) of each gene are represented between 8-cell stage and blastocysts.

(b) A table summarizing the total differentially expressed (DE) genes between CB *wt* and CB *Xist*^{patΔ} female embryos during early development and their localization on X chromosomes or autosomes. The percentages shown correspond to the distribution of total DE genes between autosomes and X chromosomes. The blastocyst stage is highlighted in red and candidate DE genes from this stage have been analyzed in Figure 4. List of DE genes is available in Supplementary Data Set 2.